Lawrence Berkeley National Laboratory
Recent Work

Title
Dynamic Covalent Chemistry for Synthetic Molecular Machines

Permalink
https://escholarship.org/uc/item/8582f611

ISBN
9781119075639

Authors
Liu, Yi
Leung, Ken C-F

Publication Date
2017-11-29

Peer reviewed

eScholarship.org Powered by the California Digital Library
University of California

Dynamic Covalent Chemistry for Synthetic Molecular Machines

Yi Liu[a] and Ken C.-F. Leung[b]

[a]The Molecular Foundry, Lawrence Berkeley National Laboratory, One Cyclotron Road, Berkeley, CA 94720, USA
[b]Department of Chemistry, The Hong Kong Baptist University, Kowloon Tong, Kowloon, Hong Kong SAR

Table of Contents

1. Introduction

Driven by the need of miniaturization, research on molecular machines has received considerable attentions as a concept transfer from the macroscopic world to the nanoscale.[1-4] Molecular machines are dynamic molecular systems, usually containing multiple movable components, the locations of which can be altered to generate motion-like conformational or configurational changes by external stimuli such as chemical, electrochemical or photochemical inputs. Each molecular machine represents a chemical device that can perform a specific function. Nature has evolved many kinds of biomolecular machines.[5] Recently synthetic molecular objects with increasing topological and functional complexity have been designed and synthesized, with the aim to rival these in living systems. Bistable mechanically interlocked molecules (MIMs),[1,6] such as [n]catenanes and [n]rotaxanes (n>1), are among the most representative types of synthetic molecular machines (Figure 1), which refer to molecular systems with two ring components or one ring and one dumbbell component, respectively, interlocked with each other by mechanical bonds. The relative movement of the rings in [2]catenanes gives rise to circumrotary motions, while in the case of [2]rotaxanes, linear sliding motions can be generated from the relative movement between the ring and dumbbell component. In both

cases, the relative ring-to-ring and ring-to-dumbbell locations are dictated at large by a variety of noncovalent bonding interactions.

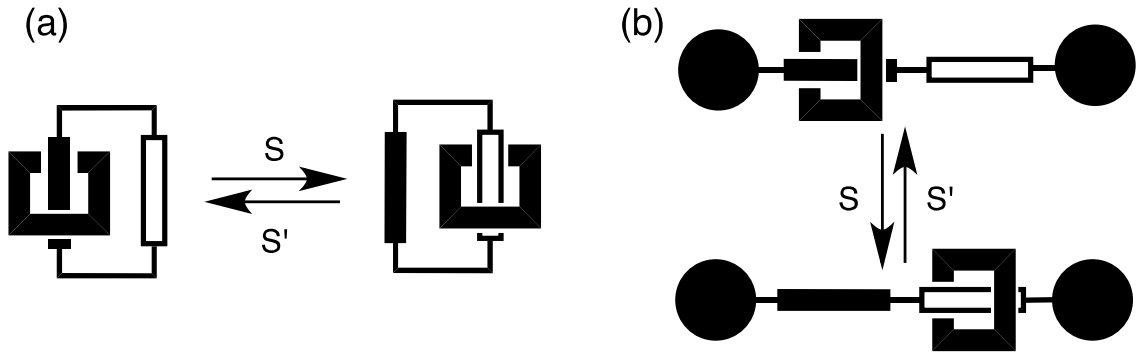

Figure 1. Molecular machines based on (a) a bistable [2]catenane and (b) a bistable [2]rotaxane.

The success of the development of versatile synthetic molecular machines essentially lies in the advancement of better understanding of strong and weak inter- and intramolecular interactions. Supramolecular chemistry,[7-9] which deals with noncovalent interactions such as hydrogen and halogen bonding interactions, π-π stacking interactions, electrostatic interactions, metal-ion binding, and solvent-solute interactions, has been utilized extensively to achieve pre-organization of molecular components for subsequent covalent linkage. Such a synthetic strategy that harnesses the power of molecular recognition and self-assembly is known as template-directed synthesis, which takes advantage of both thermodynamic and kinetic characteristics of classical noncovalent and covalent bonding interactions. Recently, dynamic covalent chemistry (DCC),[10-13] which combines the thermodynamic reversibility of noncovalent interactions,

and the kinetic stability of covalent interactions, has emerged as a powerful tool for target-oriented synthesis of topologically complex molecules[14] or diversity-oriented synthesis of dynamic constitutional libraries (DCL). [15-17] When combining noncovalent templating with dynamic covalent chemistry, the two levels of reversibility give rise to a remarkably versatile, equilibrium-based pathway towards high-yield syntheses of topologically interesting structures that are inaccessible by conventional covalent approaches. Various DCC chemistries, such as imine chemistry, disulfide exchange, boronic ester linkage, and olefin metathesis, have been routinely exercised in the synthesis of sophisticated mechanically interlocked molecules, including these possessing bistability. The introduction of DCC within bistable molecular machines also offers new opportunities for modulating the switching behavior between different states. In conventional molecular machines, the relative locations of different components are held by noncovalent interactions. When DCC is used instead of noncovalent interactions, the covalent characteristics bring about more distinctive states as a result of larger energetic separations, implying more stable machine-like operations.[18]

In this chapter, we will summarize molecular machine-related dynamic covalent chemistry in two categories: molecular machines that are assembled by DCC chemistry, and these that are operated by DCC chemistry. In the first category, we will highlight some

representative DCC chemistry that have been recognized for their high efficacy and selectivity in the assembly of interlocked molecules, particularly these that can function as switchable systems. The general utilization of DCC for interlocked molecules has been extensively reviewed and is not the focus of this chapter.[19] In this category we will also introduce several examples of DCC-based non-interlocked molecular machines. The second category summarizes molecular machines that utilize dynamic bond formation and breakage to govern the switching between different states. At the last part of the chapter a perspective on DCC and molecular machines is offered.

2. Molecular Machines Assembled by Dynamic Covalent Chemistry

In the following section, representative examples of switchable molecules are presented, including interlocked molecules and non-interlocked rotary molecular machines, all based on dynamic covalent bonds.

2.1. Mechanically Interlocked Molecular Machines

2.1.1 By Imine Chemistry

One of the most common strategies in applying DCC for interlocked molecules is the so-called “clipping” method,[20] which involves the

linkage of different partial macrocyclic components that are pre-organized around a template. This strategy has been extensively exercised in imine-based synthesis of interlocked molecules. Stoddart and coworkers have pioneered the hydrogen-bonding mediated imine assembly from mixing bis(3,5-dimethoxybenzyl)ammonium hexafluorophosphate **1** with a solution of equimolar of 2,6-pyridinedicarboxaldehyde **2** and tetraethylene glycol bis(2-aminophenyl)ether **3** (Figure 2a).[21] The desired [2]rotaxane **4** was obtained quantitatively in a few minutes. The high efficiency of the clipping reaction was the basis for the successful synthesis of monodisperse oligo[n]rotaxane **6** (Figure 2b). Multiple dialkylammonium centers, such as these in **5**, were incorporated into the dumbbell component and subjected to clipping with dialdehyde **2** and diamine **3**. Monodisperse oligo[n]rotaxanes with n up to 15 were obtained in high yield when dibenzylammonium centers were used, thanks to positive cooperativity arising from extended π-π stacking interactions.[22,23]

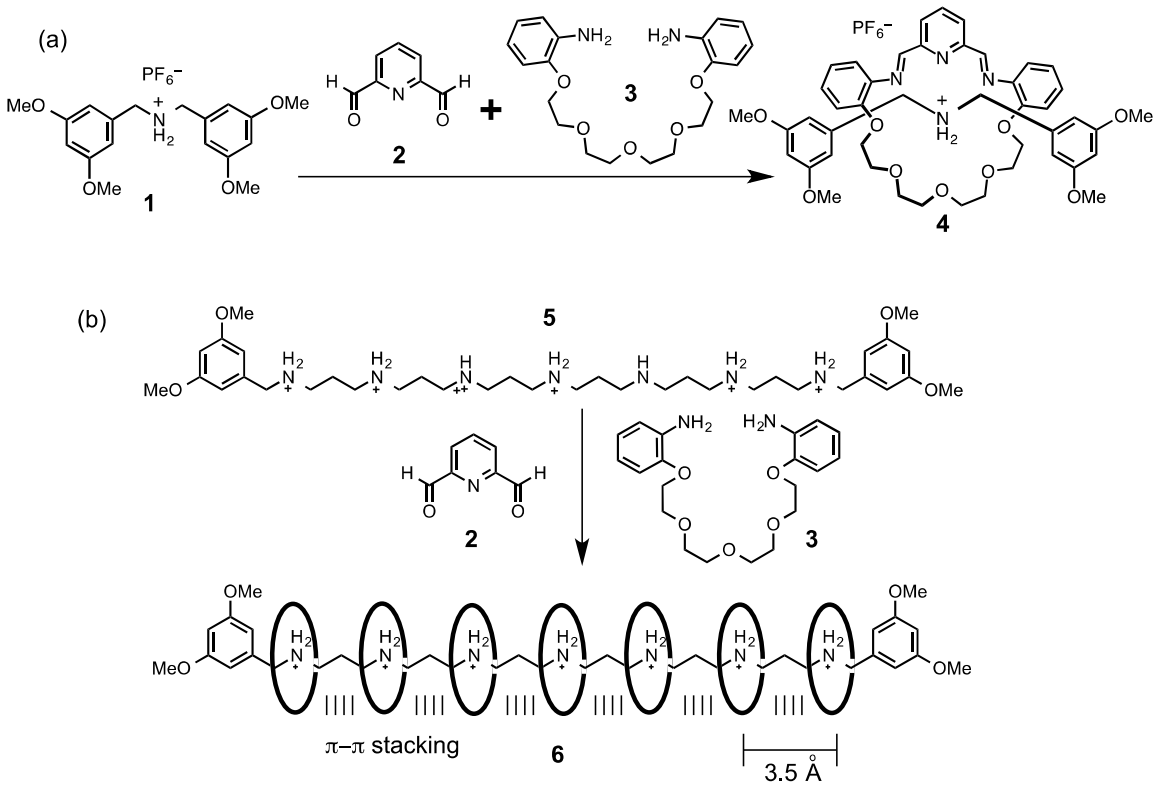

Figure 2. The hydrogen-bonding templated clipping of (a) a [2]rotaxane and (b) [n]rotaxanes.

The imine-based clipping reaction has been utilized by Tatay and coworkers in the synthesis of switchable copper-complexed interlocked systems.[24] By reacting dumbbell-shaped component **7** with diamine **8** and 2,6-diformylpyridine (**2**) in the presence of $Cu(MeCN)_4PF_6$, followed by reduction of the diimine gave rise to [2]rotaxane **9-Cu(I)** (Figure 3). As evidenced by electron spin resonance spectroscopy and cyclic voltammetry, the introduction of such a pyridine bisamine moiety, which replaced the classical terpyridine terdentate unit, led to significant stabilization of the penta-coordinated Cu(I) site. Upon oxidation of Cu(I) to Cu(II), pirouetting of the macrocycle was activated

to favor the formation of a tetra-coordinated Cu(II) complex between the two phenanthroline units. Such an electrochemical switching process took place at the millisecond timescale, which represented the fastest switching rotaxane in Cu-based interlocked dynamic systems. The DCC chemistry incorporated here not only showcases the synthetic simplicity, but also has led to a bistable system with more distinct energetic separation between states and an acceleration of the reorganization processes.

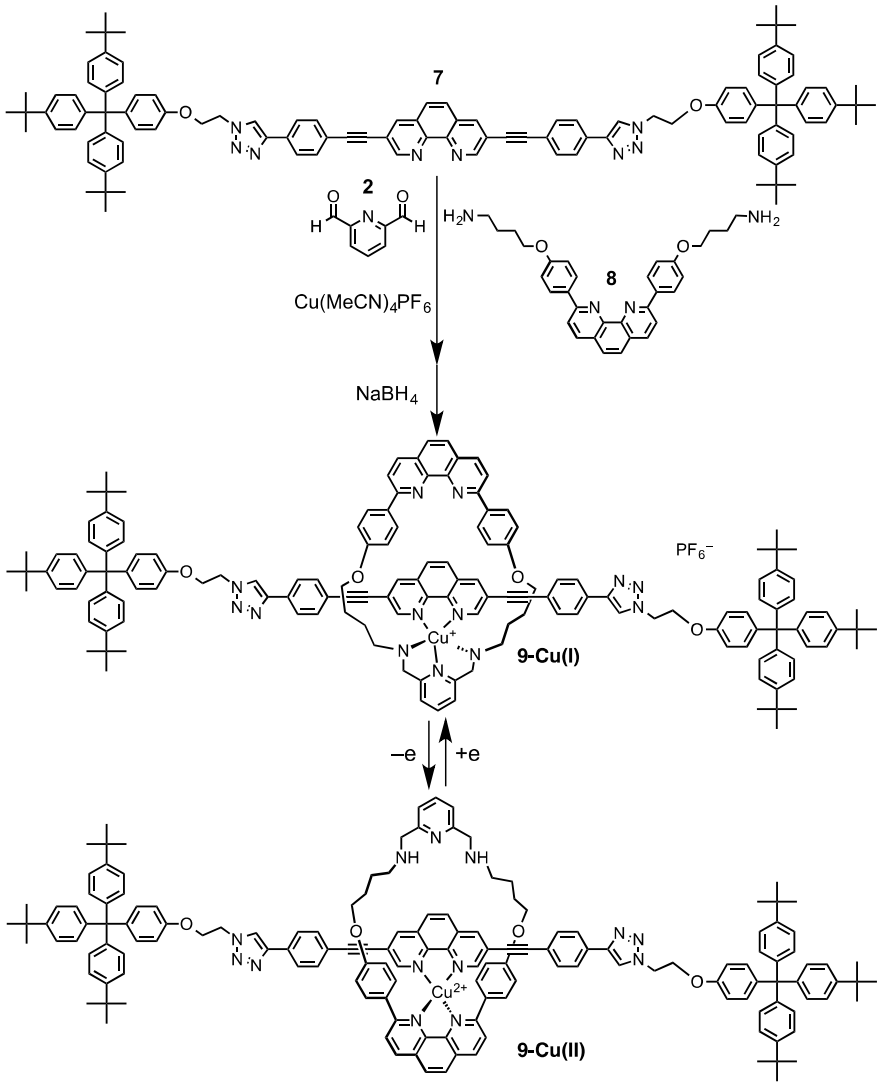

Figure 3. A bistable [2]rotaxane synthesized by imine clipping reaction, and the related redox activated switching between penta-coordinated and tetra-coordinated Cu centers.

Similar imine clipping reaction has also been employed in the synthesis of photoswitchable [2]catenanes **10**, one macrocyclic component of which contains an ammonium center for templated clipping of another macrocycle and a photoresponsive dithienylethene (DTE) unit (Figure 4).[25] Good photochromic reversibility and excellent fatigue resistance were observed as a result of the formation of open and closed isomers of the DTE unit upon UV or visible light irradiation. The catenation of the imine-based macrocycle on the macrocyclic ammonium salt rendered enhanced photochromic properties compared with these of the ammonium salt containing macrocycles alone.

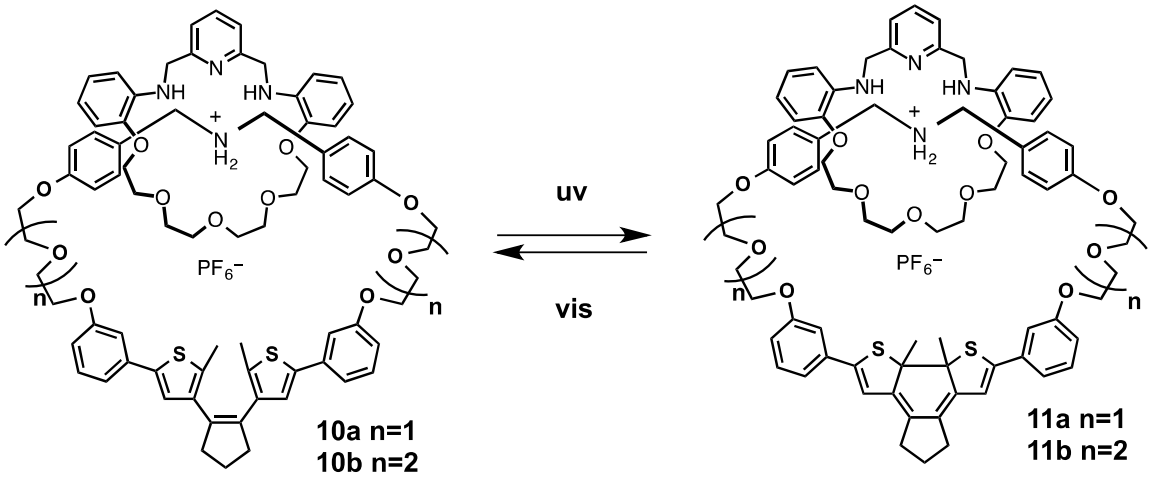

Figure 4. Switchable [2]catenanes containing a photoresponsive dithienylethene unit.

The facile imine bond formation also facilitates the synthesis of an anthracene-containing dynamic [2]rotaxane **AnthR-H**·PF_6, which behaved as an acid sensor as well as molecular logic device based on the fluorescence response of the anthracene end group (Figure 5).[26] The [2]rotaxane **AnthR-H**·PF_6 was prepared by the aforementioned "clipping" approach by reacting dialdehyde **2**, diamine **3**, and a dumbbell shaped secondary dialkylammonium ion (**Anth-H**·PF_6 template). Owing to the complementary recognition associated with [$N^+H\cdots O$] and [$N^+CH\cdots O$] hydrogen bonds as well as electrostatic and π-π interaction between the macrocycle and dumbbell component, the thermodynamically stable dynamic [2]rotaxane was obtained in high yield (>90%), without formation of other higher-order macrocyclic homo-oligomers or acyclic oligomers. Furthermore, the anthracene fluorescence of the [2]rotaxane could be completely quenched by electron transfer from the imine and pyridine moieties in the macrocycle in close proximity. In addition, it is known that the imine bonds in macrocycle are responsive to the presence of water, acid, salt (KPF_6) and amine (*p*-toluidine). Two acid sensors (HCl/H_2O) and (HCl/Et_2O) had been identified with different modes of dimmer control —that is, logarithmic and linear. The use of a combination of stimuli for the [2]rotaxane was summarized in the table of Figure 5, employing a binary notation with four different inputs and one output. Noticeably, the output entries C, I, J, and O were somewhat uncertain since it was

difficult to reach thoroughly dry conditions. If the situation relating to the residual water molecules present in the solutions was overlooked, then the outputs could be interpolated (as the bracketed values). Since the fluorescence signal could be observed by various input or stimuli, different molecular logic had been realized by rational selection of different combinations of input.

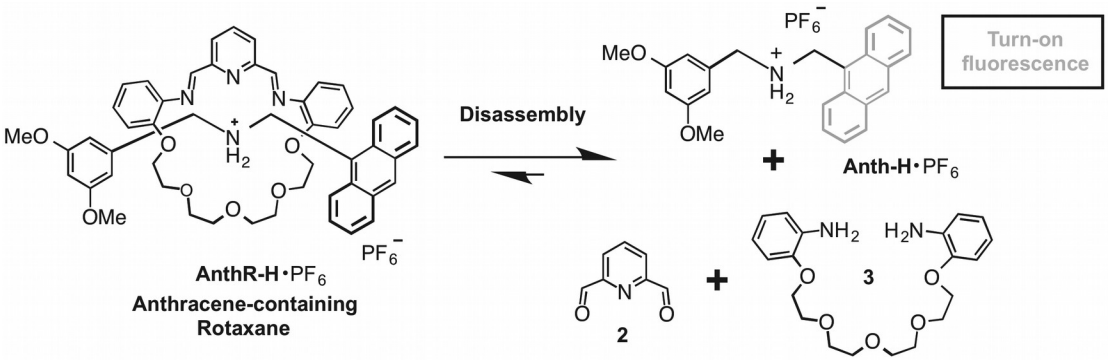

entry	input				output	
	H_2O	**H^+**	**KPF_6**	**Tol-NH_2**	**anthracene fluorescence (418 nm, excitation = 290 nm)**	**fluorescence at 330 nm (excitation = 290 nm)**
A	0	0	0	0	0	1
B	1	0	0	0	0	1
C	0	1	0	0	(1)	(0)
D	0	0	1	0	0	1
E	0	0	0	1	0	1
F	1	1	0	0	1	0
G	1	0	1	0	0	1
H	1	0	0	1	0	1
I	0	1	1	0	(1)	(0)
J	0	1	0	1	(1)	(0)
K	0	0	1	1	0	1
L	1	1	1	0	1	0
M	1	1	0	1	1	0
N	1	0	1	1	0	1
O	0	1	1	1	(1)	(0)
P	1	1	1	1	1	0

Figure 5. Dissociation of anthracene-containing rotaxane **AnthR-H**·PF_6 with “turn-on” fluorescent properties and summary of the fluorescence

output of the rotaxane **AnthR-H**·PF_6 in the presence of four different additive inputs (H_2O, H^+, KPF_6, and Tol-NH_2). Input: "1" represents the presence of the additive while "0" represents the absence of the additive. Output: "1" represents observable fluorescence while "0" represents no observable fluorescence (fluorescence quenched). The output entries C, I, J, and O (parentheses) are somewhat uncertain since thoroughly dry conditions are difficult to realize.

Other types of noncovalent interactions, such as donor-acceptor interactions, have also been utilized in dynamic clipping of interlocked molecules. In the presence of an electron deficient π-template, such as the bipyridinium (**BPY**)-containing dumbbell-shaped compound **12**, a six-component [2+3] clipping reaction that involves two equiv. of 1,3,5-benzenetrialdehyde (**13**) and three equiv. 2,2'-(ethylenedioxy)diethylamine (**14**) (Figure 6a), works efficiently to afford the desired [2]rotaxane **15** as the single product.[27] Weak interactions, the main one being π-π interactions between the **BPY** template and the macrobicycle, contributed to the overall stabilization of the threaded product, despite a symmetry mismatch between the host and the guest. Recently, c_3-symmetric trispyridinium (**TPY**) guests, such as **16** in Figure 6b, was also employed as an effective template for the formation of a triply-threaded [2]rotaxane **17**.[28]

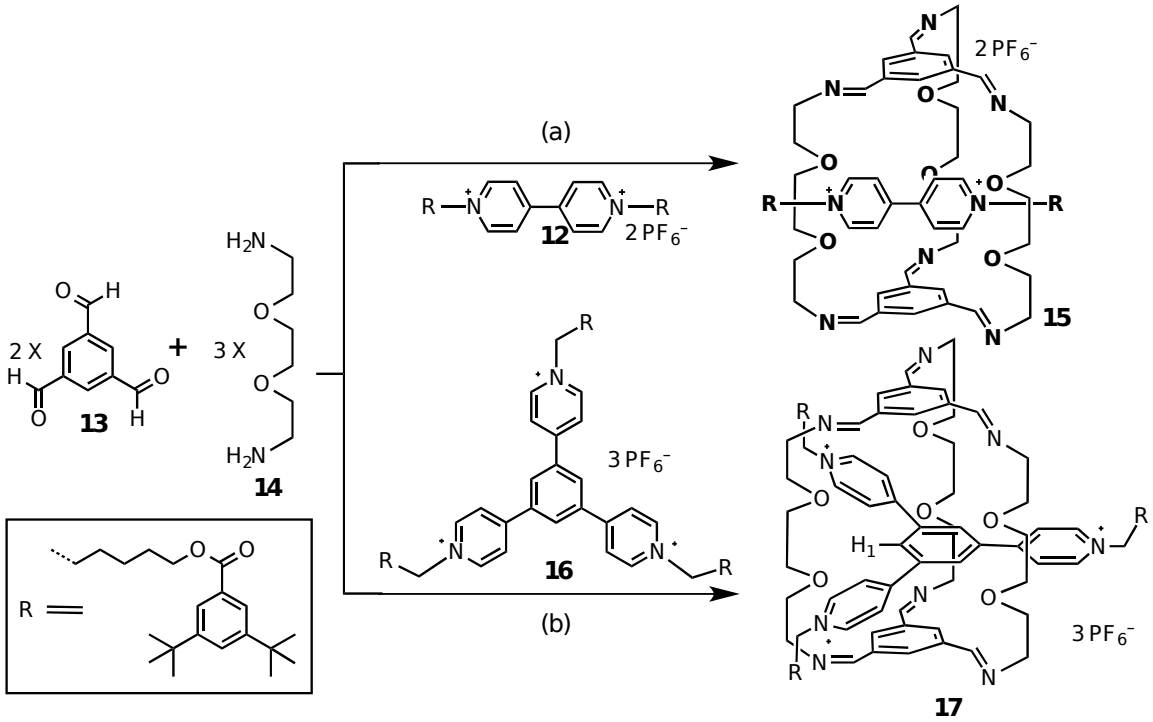

Figure 6. Templated dynamic clipping for the formation of [2]rotaxanes by (a) a linear and (b) a c_3-symmetric template.

The difference of templating power between **BPY** and **TPY** units renders an unconventional solvent dependent switching between the two [2]rotaxanes **15** and **17** (Figure 7).[29] In competition clipping experiments employing both **BPY** and **TPY** as the templates, exclusive formation of the **BPY**-based linear [2]rotaxane **15** could be achieved in pure $CDCl_3$, while in pure CD_3CN, a 6.7:1 selectivity was achieved in favor of the **TPY**-based triply threaded [2]rotaxane **17**. Such an environmental responsive switching between different structures was related to the subtle differences of the aromatic-aromatic interactions that govern the templated formation of two [2]rotaxanes. The **BPY**-based clipping reaction was driven by electrostatic interactions

between aromatic surfaces, while the **TPY**-based reaction was driven by solvophobic interactions. It is the difference in the collective noncovalent interactions that accounts for the opposite selectivity in different chemical environments, which can be essential for the design of complex molecular architectures that greatly relies on weak but cooperative noncovalent interactions.

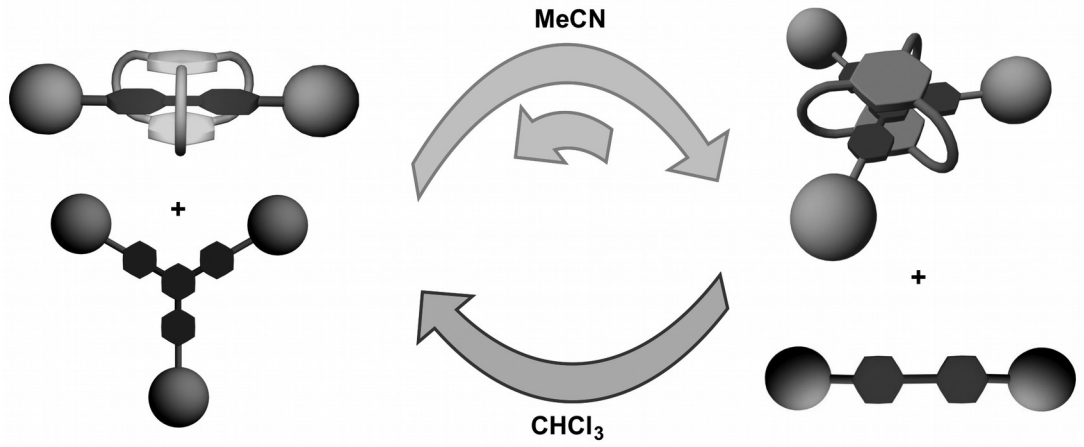

Figure 7. Illustration of dynamic switching between a linear [2]rotaxane and a triply threaded [2]rotaxane in response to different solvent conditions.

The dynamic clipping approach combining π-templating and reversible imine chemistry has also been applied in the preparation of [2]catenanes (Figure 8).[30] A mixing of terephthaldehyde (**18**), 2,2'-(ethylenedioxy)diethylamine (**14**), and the tetracationic cyclobisparaquat (**19**) ($CBPQT^{4+}$) in CD_3CN in 2:2:1 ratio resulted in the formation of a single species that corresponded to the [2]catenane **20**. No [2]catenane was formed when 1,5-diformylnaphthalene (**21**) was used instead of terephthaldehyde. Interestingly, when equimolar of **18**

and **21** were mixed with diamine **14** (2 equiv) and cyclophane **19** (1 equiv), an unsymmetrical [2]catenane **22** was formed selectively as the major product in 90% yield, together with ~5% of the symmetric [2]catenane **20**. Furthermore, only one translational isomer of **22** was observed both in solution and in the solid state, with the diiminobenzene ring system sitting inside the cavity of the tetracationic cyclophane and the diiminonaphthalene ring system sitting alongside. Steric effects, together with strong π-π interactions between the aromatic units and the collective [C-H···O] interactions in a molecular geometry with ideal preorganization are responsible for high selectivity expressed in the clipping reaction. This approach offers a thermodynamic pathway to desymmetrized [2]catenanes by installing different recognition units in one simple step in one of the macrocyclic components, which holds great promises for the construction of switchable molecules with multistability.

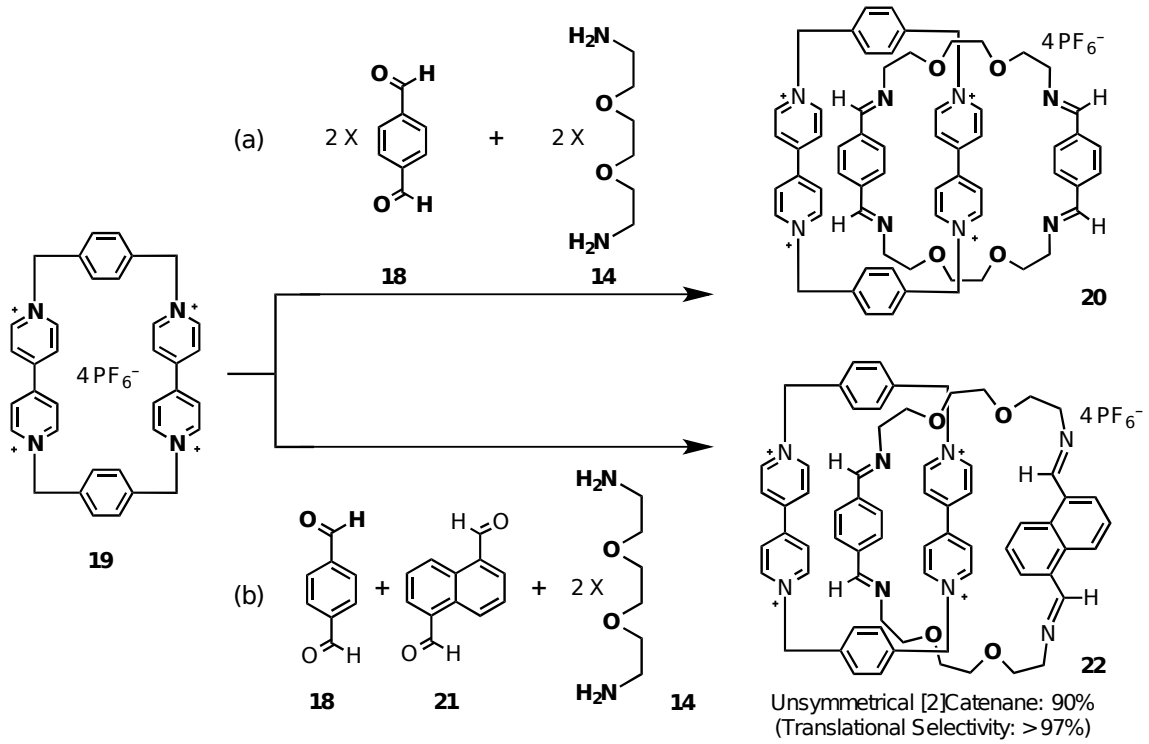

Figure 8. Templated dynamic clipping for the selective formation of [2]catenanes.

2.1.2. By Disulfide Bond Formation

Sanders and coworkers have detailed the construction of dynamic covalent library (DCL) based on reversible S-S bond formation in aqueous solution,[31-36] from which donor-acceptor type [n]catenanes were identified and amplified.[32,35] For example, an aqueous disulfide DCL was derived from a mixture of an electron accepting naphthalene diimide (NDI) derivative **23** and an electron donating dioxynaphthalene (DNP) derivative **24** that was equilibrated under air oxidation (Figure 9). It was found that the formation of donor-acceptor [2]catenane **25** was amplified by increasing the concentrations of each building blocks, or under high ionic strength. [2]Catenane **25** consisted of two identical

macrocyclic components, each containing one DNP and one NDI ring systems that were covalently linked by S-S bond. Different from the conventional alternating donor-acceptor stacking geometry, it adopted a donor-acceptor-acceptor-donor stacking conformation, likely a consequence of enhanced hydrophobic interaction that compensated the diminished electrostatic interactions. The use of an electron rich cationic template **26** could also amplify the formation of [2]catenane **25** by intercalating between the two electron deficient NDI moieties, giving rise to a supramolecular assembly featuring five alternating donor and acceptor units. The construction of such an unusual donor-acceptor [2]catenane from acyclic precursors manifests the power of dynamic covalent chemistry. A more detailed mechanistic study of the formation pathways of different donor-acceptor [2]catenanes,[37] as well as the formation of more complex [3]catenanes[35] were reported based on similar constitutional DCLs.

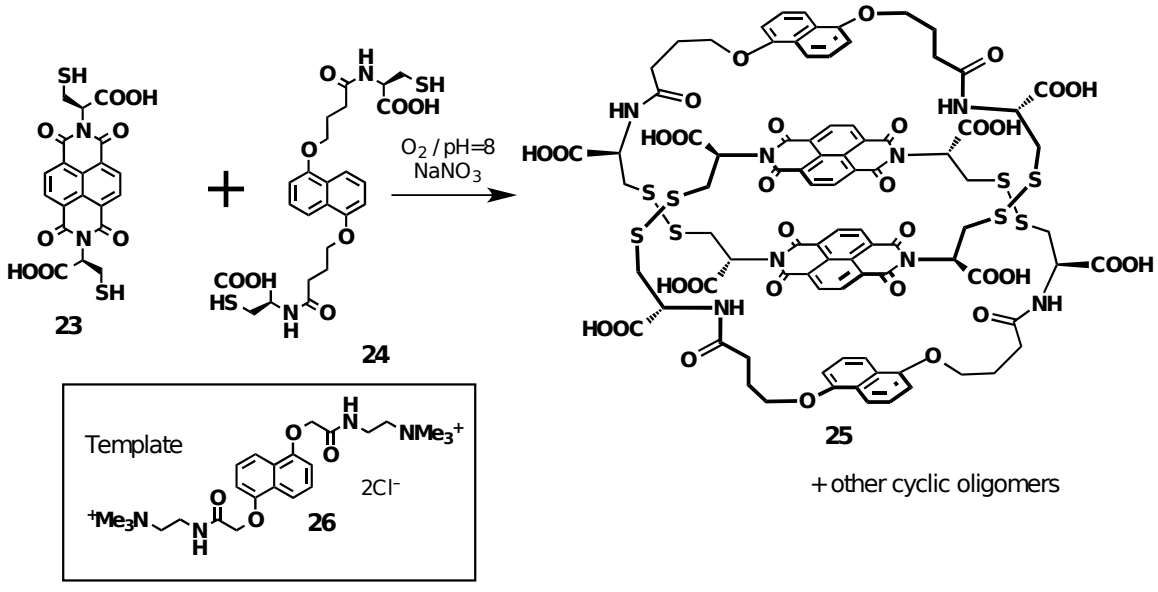

Figure 9. Formation of a covalent donor-acceptor [2]catenane **25** from a dynamic covalent library with electron acceptor **23** and electron donor **24**. The structure of an electron-donating template **26** for product amplification was also illustrated.

The power of DCC chemistry also enables the discovery of a conformationally switchable donor-acceptor [2]catenane **28** from a dynamic combinatorial library. The reaction was carried out in water in a similar fashion to the synthesis of [2]catenane **25**, involving the same electron acceptor **23** and a slightly modified electron donor **27** (Figure 10a), which differed from **24** by the substitution pattern on the DNP ring system (2,6- instead of 1,5-substitution).[34] Unlike [2]catenane **25**, two *co*-conformations were observed in the new [2]catenane **28**. While one of the conformations was the conventional coplanar donor-acceptor stack, the other one featured an unprecedented arrangement of the π systems, in which the flat NDI π-surfaces were vertically stacked in parallel with each other to give a shape that was reminiscent of the astrological Gemini sign (Figure 10b). Switching between the parallel and nonparallel conformations could be achieved by manipulating temperature, solvent polarity, or by the addition of the guest **26**. Raising the temperature or introduction of **26** favored the formation of the coplanar conformation, while decreasing the solvent polarity by adding acetone into water favored the formation of the Gemini conformation. The discovery of such an unconventional

switchable system is another example that highlights the versatile role of DCC in the discovery of compounds with unexpected structural features.

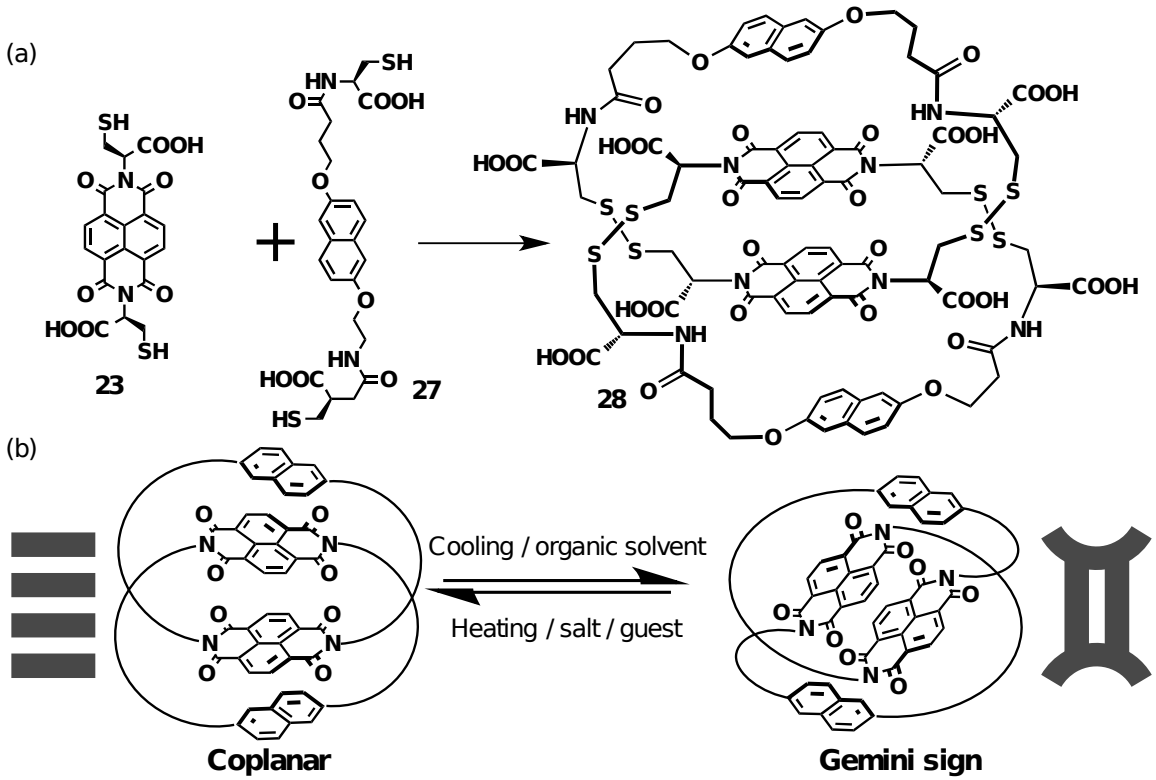

Figure 10. (a) Synthesis of a donor-acceptor [2]catenane **28** that is able to (b) switch between a conventional parallel and an unconventional nonparallel conformation.

2.1.3 By Olefin Metathesis

The development of ruthenium−alkylidene complexes-catalyzed olefin metathesis has marked another major advance for the synthesis of interlocked molecules, including [2]rotaxanes,[38,39] [2]catenanes,[40,41] and

multiply threaded species.[42-45] For example, ammonium binding has been utilized as the templating strategy to build triply thread [2]rotaxanes[42] and [2]catenanes[44] in high yields after threefold metathesis. As shown by Chen and coworkers, the D_{3h} symmetrical triptycene tris(crown ether) host **29** formed a complex with three equivalent of olefin-terminated dibenzylammonium (DBA) salt **30**, which, after olefin metathesis catalyzed by Grubbs' second-generation catalyst and subsequent hydrogenation, gave the triply threaded [2]catenane **31** in high yield (Figure 11). Such multifold, templated metathesis has also been utilized in the synthesis of molecular trefoil knots,[46,47] and David's Star,[48] as pioneered by Sauvage and Leigh, respectively.

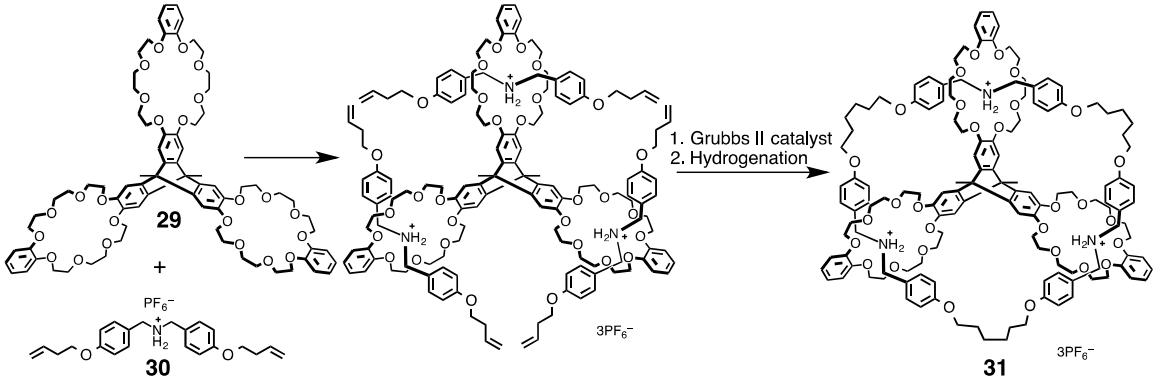

Figure 11. Synthesis of a triply threaded [2]catenane by olefin metathesis.

Chen and coworkers recently utilized the dynamic ring-closing olefin metathesis to build a triply interlocked [2]catenane **34** that could undergo stepwise rotary motion.[49] Built on their earlier success on the synthesis of the D_{3h} symmetrical host **29**, they designed and

synthesized a pyrazine-extended triptycene-derived tris(crown ether) **32** that had more free volume to accommodate three new recognition sites on the inner threading component (Figure 12). The threading component **33** was constructed to contain three DBA and three methyltriazolium (MTA) recognitions sites for dibenzo-24-crown-8 (DB24C8) and two alkenyl ends. Complexation between **32** and **33** occurred readily upon mixing, from which the [2]catenane **34** was obtained in 83% yield after treatment with a catalytic amount of Grubbs' second-generation catalyst and subsequent hydrogenation. The presence of multiple nondegenerate recognition sites in **34** rendered distinctive stepwise molecular motions during acid-base triggered switching process, as all four *co*-conformations could be clearly identified by ^{1}H NMR titration experiment. Upon deprotonation with 1,8-diazabicyclo[5.4.0]undec-7-ene (DBU) of the first ammonium center in **34**, the surrounding crown ether left the DBA site to bind the nearest MTA site in the partially deprotonated **35** (Figure 12b). The next deprotonation event of another DBA center activated the movement of the second DB24C8 arm to the nearby MTA site in **36**. Similar crown ether displacement was triggered during the final deprotonation of the third DBA center in **37**. All these processes could be reversed by the controlled addition of trifluoroacetic acid (TFA). It should be noted that the two MTA sites next to the same DBA site in the cyclic thread were spaced differently, which endowed unexpected

selectivity due to the specific interlocked topology, with the one closer to the DBA site being the more favorable one after each protonation step. This study opens new windows for the design of artificial molecular machine with excellent mechanochemistry properties, the underlying motion mechanism of which could provide more insights to intricate biological molecular machines.

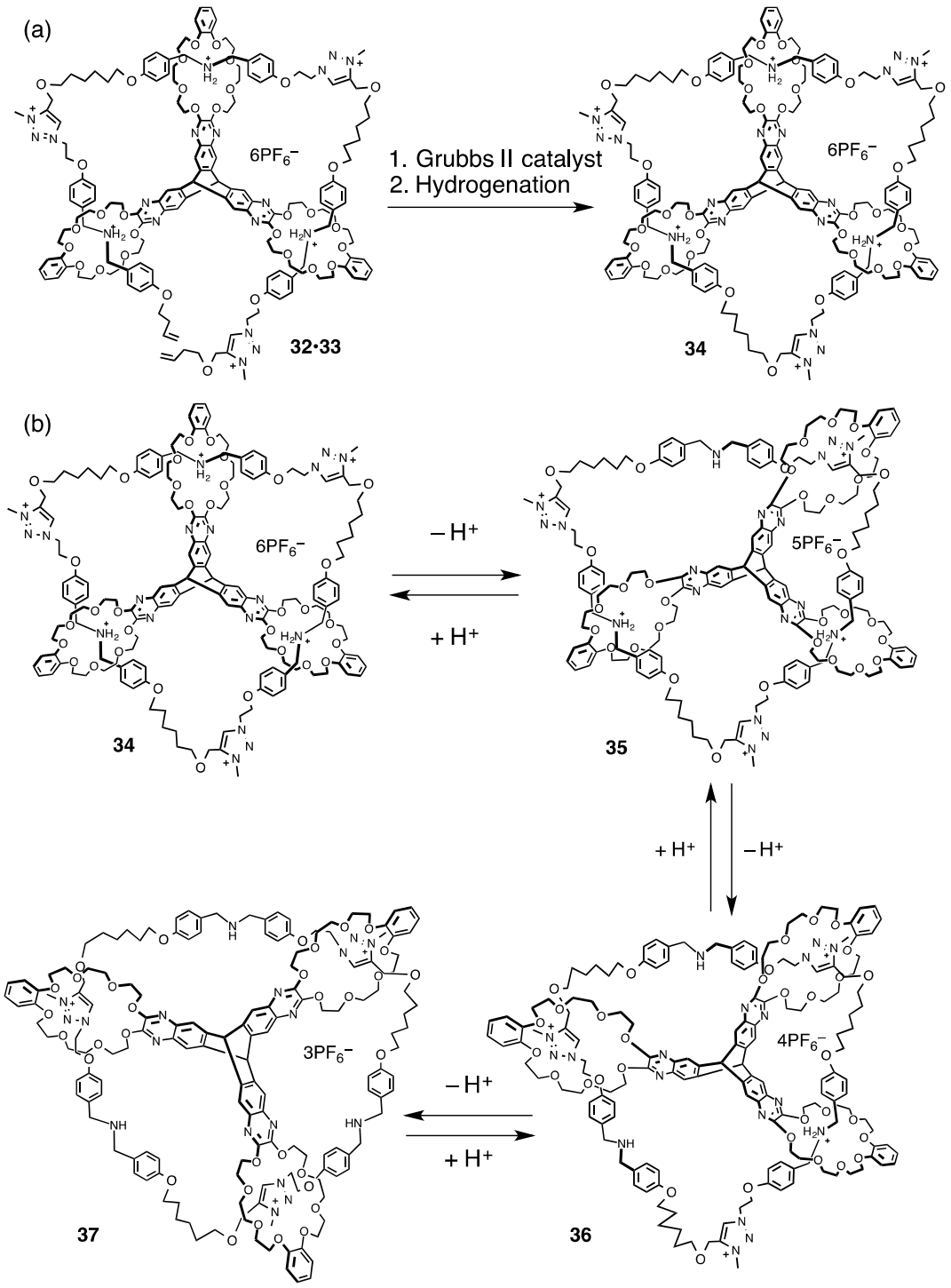

Figure 12. (a) Synthesis of the triply interlocked [2](3)catenane **34** by olefin metathesis from the pseudorotaxane precursor **32•33**. (b) Illustration of the stepwise acid-base triggered switching process.

2.1.4 By Iodide-Catalyzed DCC

Stoddart and coworkers have employed an unusual thermodynamically controlled S_N2 reaction for the construction of switchable molecular motors by magic-ring like experiment. This was demonstrated in the iodide-catalyzed catenation from two preformed covalent macrocycles, i.e., an electron-deficient cyclobis(paraquat-*p*-phenylene) ring (**19**) and an electron-rich crown ether **38a** containing two dihydroquinone (HQ) units. Nucleophilic iodide attack of the benzylic carbons in **19** at 80 °C resulted in its ring opening (Figure 13), leaving a linear molecule **39** that had less ring strain than the parent cyclophane. A pseudorotaxane was formed between **39** and the electron-rich crown ether by favorable host-guest interactions. Reverse S_N2 reaction between the free pyridine and the benzylic iodide regenerated the bisparaquat macrocycle, concurrent with formation of the interlocked [2]catenane **40a** in 46% isolated yield. The equilibrium was biased towards the side of [2]catenane because of the stabilizing π-donor–π-acceptor interactions between the two rings. The use of more electron-rich 1,5-dinaphtho[38]crown-10 (**38b**) proved advantageous, rendering the equilibrium virtually completely on the [2]catenane side and a much higher isolated yield of 93%. This dynamic reaction was applied on the synthesis of bistable switchable [2]catenane **40c**[50] using this “magic ring” protocol. Under conditions

identical to those used in the synthesis of **40a** and **40b**, **40c** was isolated in 60% yield, which was almost three times greater than that observed (23%) by using conventional kinetically controlled reaction conditions.

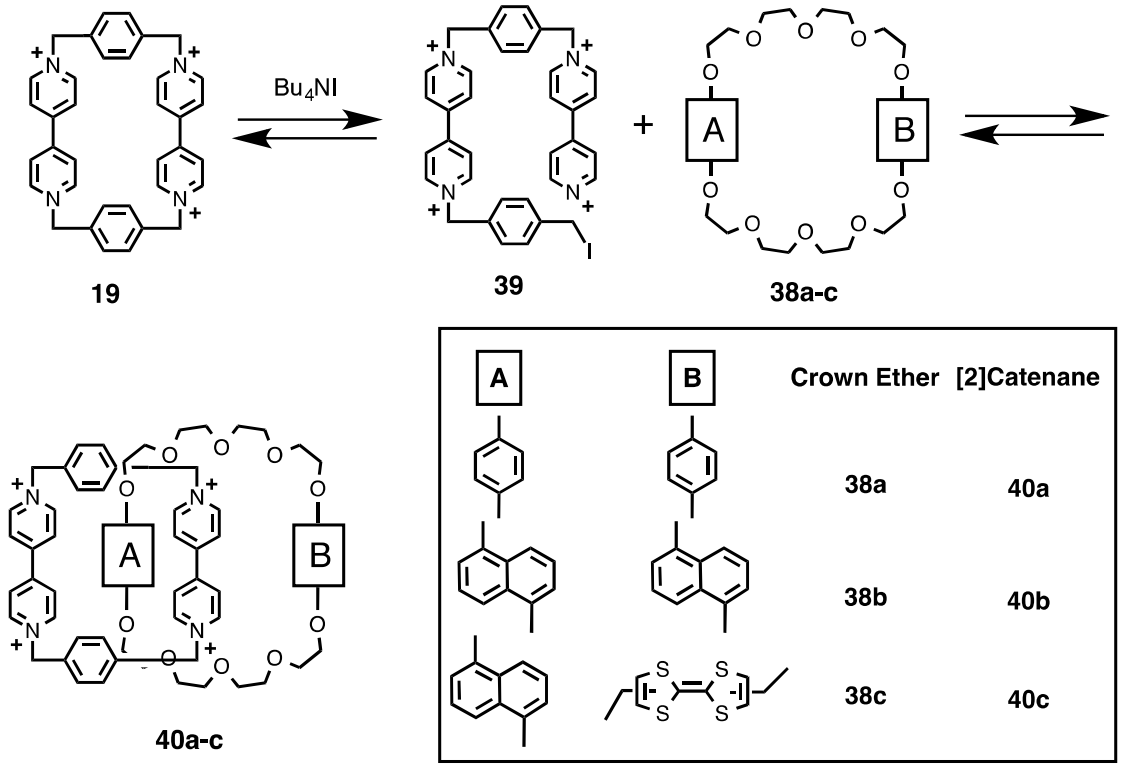

Figure 13. Iodide mediated ring-opening and ring-closing equilibrium that facilitate the formation of donor-acceptor [2]catenanes.

2.2. Non-Interlocked Molecular Machines

Synthetic rotary molecular machines based on systems other than interlocked molecules can be accomplished by utilizing configurational isomerization of double bonds, such as *cis/trans* isomerization of C=C bond demonstrated in chiral helical molecules.[51] The dynamic C=N

double bond in imines and hydrazones could undergo similar isomerization and be utilized in a similar way to generate configurational and conformational changes through a sequence of chemical operations.

2.2.1 Imine-Based Motors

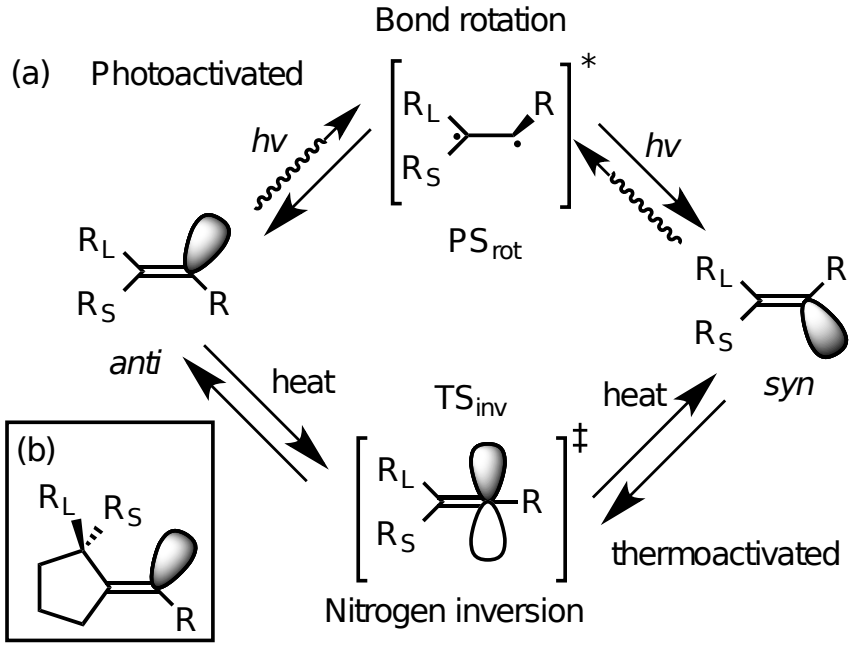

Figure 14. (a) Illustration of two different pathways of configurational switching in imine through out-of-plane bond rotation (PS_{rot}) or in-plane nitrogen inversion (TS_{inv}). (b) A design of imine containing symmetry-breaking chiral unit as a candidate for preferred unidirectional rotation. R_L and R_S represent larger and smaller substituents.

As conjectured by Lehn,[52] imines and similar C=N based class of molecules, can function as the simplest rotary motor. Two energetically biased processes are associated with configurational

imine isomerization, namely, photochemically driven rotation and thermally activated “linear” inversion. The former process is based on a photochemical process that, upon irradiation of the imine substrate, undergoes an “out-of-plane” rotation around the C=N bond via a perpendicular excited state PS_{rot}. When two substituent groups are different (R_L and R_S represent larger and smaller substituents), such photochemical transformation may convert the thermodynamically more stable *anti* (*E*) form (R *trans* to R_L) to the less stable *syn* (*Z*) form (R *cis* to R_L). Following this photochemical process, the *syn* form can revert to the more favorable *anti* form through a thermally activated in-plane nitrogen inversion via a linear transition state TS_{inv}. Such photoinduced rotation of imines generates motor-like motions around the C-N axis with no directional selectivity. In order to incur unidirectional rotation, symmetry-breaking components, such as optically active cyclopentanone that contains a chiral carbon center close to the imine group (Figure 14b), was proposed to induce preferential rotation in one direction.

2.2.2 Imine-Based Switches

Apart from the preparation of molecular motors, imine bond can also be used for reversible switching control between hydrophilic and hydrophobic surfaces of nanoparticles (Figure 15).[53] A hydrophilic, superparamagnetic iron oxide nanoparticles (SPIO-NH_2) with amine-

functional groups can be condensed with hydrophobic, dendritic dialdehydes (Gn-CHO). From the wettability study, the SPIO-NH_2 demonstrates a water contact angle of 42° on mica surface. On the other hand, the third generation-dendronized SPIO (SPIO-G3) nanoparticles demonstrate a higher water contact angle of 85° on mica surface. Thus, the dendronization of nanoparticles through imine bond could result in a significant increase of the hydrophobicity. Actually, the hydrophobicity of the surface of the dendronized nanoparticles can be decreased by using different systems (Figure 15, inset graph) and tuned at different rate. The rate of decrease of the contact angle for SPIO-G3 is H_2O □□1% $Co(OAc)_2/H_2O$ □□DMF/H_2O (1:1), with rates of 4.0°, 2.9°, and 1.0° per min, respectively. In particular, the use of a drop of 1% $Co(OAc)_2/H_2O$ in the contact-angle measurement for SPIO-G3 gives a lower rate of decrease in the contact angle. This observation could be due to the temporary templating process between the imine groups of SPIO-G3 and the Co^{2+} cations, which slows down the dissociation/hydrolysis process, revealing a larger final contact-angle value (48°) compared to the value using H_2O (44°). On the other hand, the use of relatively less polar solvent system, DMF/H_2O (1:1), successfully reduces the dissociation rate of SPIO-G3 toward hydrolysis, with a 1.0°/min decrease of the contact angle. By removing the water molecules of the wetted SPIO-G3 nanoparticles, the surface of the nanoparticles becomes hydrophobic again with an increased

contact angle of >85°.

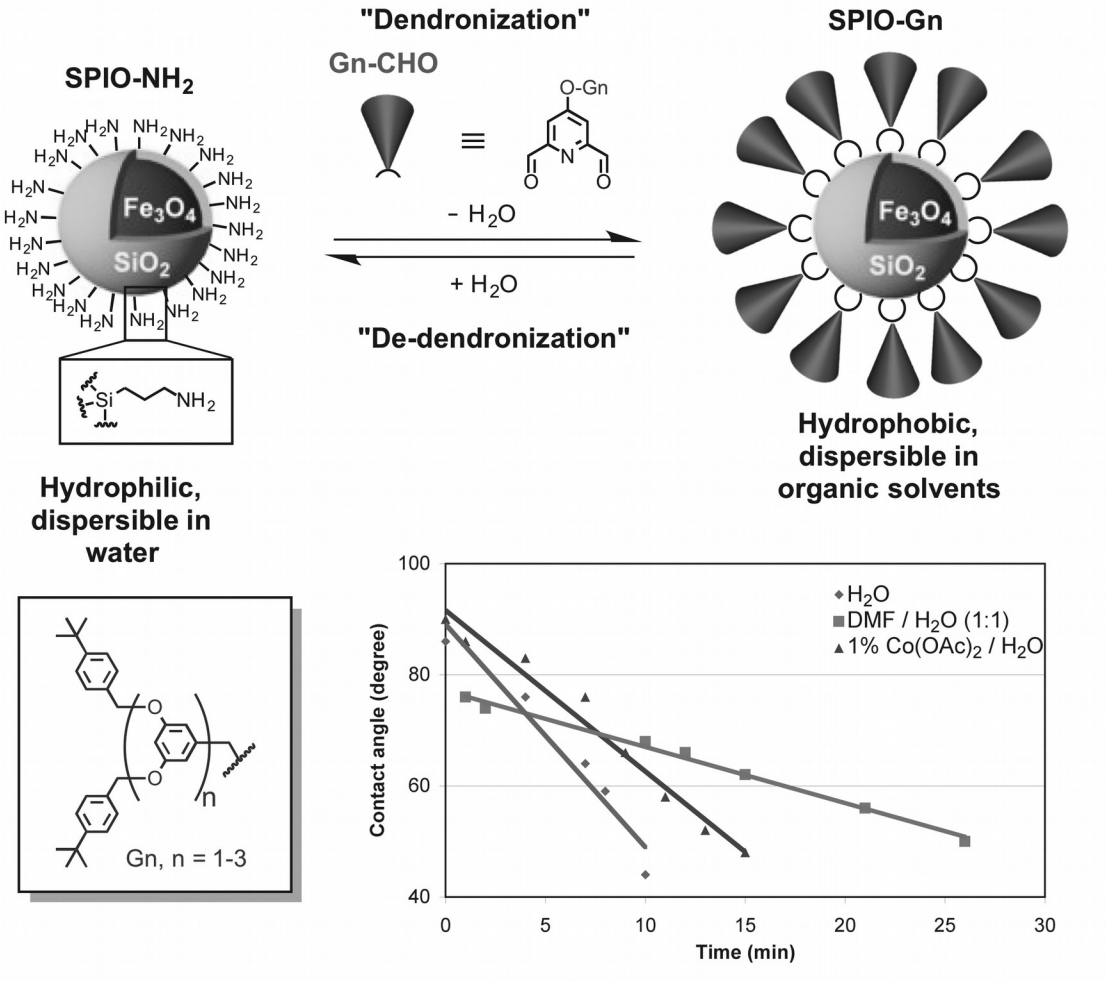

Figure 15. Graphical representation of the reversible control between hydrophilic SPIO-NH_2 nanoparticles and hydrophobic dendronized SPIO-Gn nanoparticles in the absence/presence of water. Inset graph: Plot of the contact angle (degree) versus time (min), showing the wettability of SPIO-G3 nanoparticles using a drop of H_2O, DMF/H_2O (1:1), or 1% $Co(OAc)_2$/H_2O.

2.2.3 Hydrazone-Based Switches

Aprahamian and coworkers have reported the use of substituted aryl hydrazine derivatives as simple configurational rotary switches, in which the *E/Z* isomerization about the C=N bond were mediated by pH[54,55] and/or metal ion binding.[56,57] As shown in Figure 16, hydrazones **41a/b** exist primarily as the *E* isomer at the equilibrium. Upon addition of trifluoroacetic acid, protonation of the pyridine moiety induces a rotation around the C=N double bond, corresponding to an *E* to *Z*-H^+ switching. Such switching is reversible, as the *E* isomer can be reinstated by treatment with base. Combined kinetic studies and density functional theory calculations have shed light on the switching mechanism, which is a hydrazone-azo tautomerization followed by rotation around a C–N single bond, as opposed to the more common in-plane N–N inversion mechanism or the rotation mechanism around the C=N double bond.

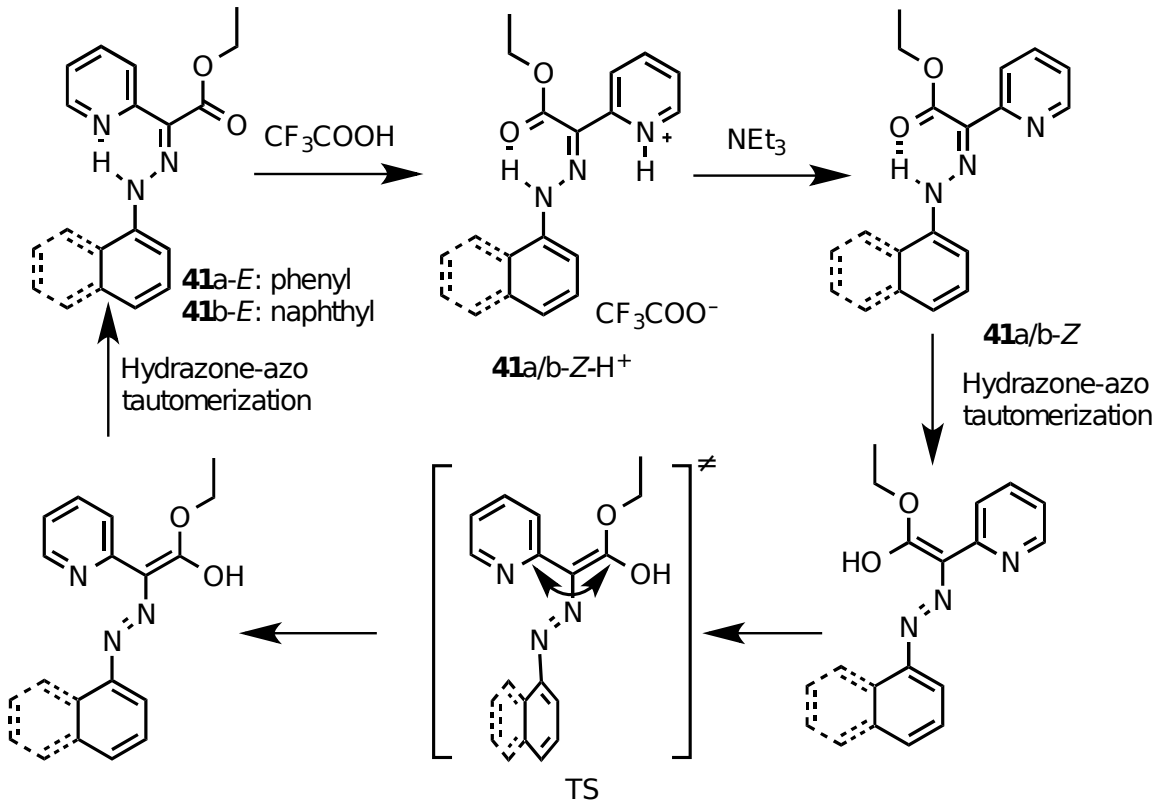

Figure 16. Acid-base induced reversible switching of hydrazone **41a/b** and the proposed switching mechanism based on hydrazone-azo tautomerization.

When a quinoline ring system was used in **41c** in replacement of the naphthyl unit (Figure 17a),[55] stepwise protonation of the pyridine and the quinoline units led to not only a similar rotation around the C=N double bond as these observed in **41a/b**, but also a conformational switching around the C–N single bond. These configurational and conformational switching occurred at each protonation events, and could be fully reverted to the ground state *E*-**41c** upon treatment with NEt_3. In addition, it was found that **41c** also

underwent *E/Z* isomerization upon treatment with Zn^{2+} through a bio-inspired coordination-coupled proton transfer mechanism (Figure 17b).[56] In this process, coordination of Zn^{2+} with hydrazone led to both C=N bond rotation and a proton transfer from the hydrazone to pyridine. This process provides a new switching mechanism in which acid modulations can be applied without the addition of protons. Indeed, this metal ion coordination induced proton transfer has proven to be a mild and neutral proton source that could be utilized to activate another hydrazone-based rotary switch as a tandem event.[57] Hydrazone **41d**, which is similar to **41c** but contains a methylimidazolyl group instead of a pyridyl one (Figure 17c), can be switched to its Zn(**41d**-*Z*-H^+) form by the addition of Zn(II) through the coordination-coupled deprotonation (CCD) mechanism. When this switching occurs in the presence of **41a**-*E*, a proton relay occurs, yielding Zn(**41d**-*Z*) and **41a**-*E*-H^+. Such a process represents a novel switching cascade triggered by a single coordination event, which is reversible upon the addition of nBu$_4$NCN. The introduction of the methylimidazolyl group is critical for such a cascade switching, which does not proceed in the case of **41c**. The unusual acidity of the imidazolyl group over pyridine, which presumably is a result of a combination of electrostatic and conformational effects, is believed to be the key to the successive proton relay steps, the study of which might help elucidate the proton-coupled electron-transfer mechanism

in photosynthetic bacteria.

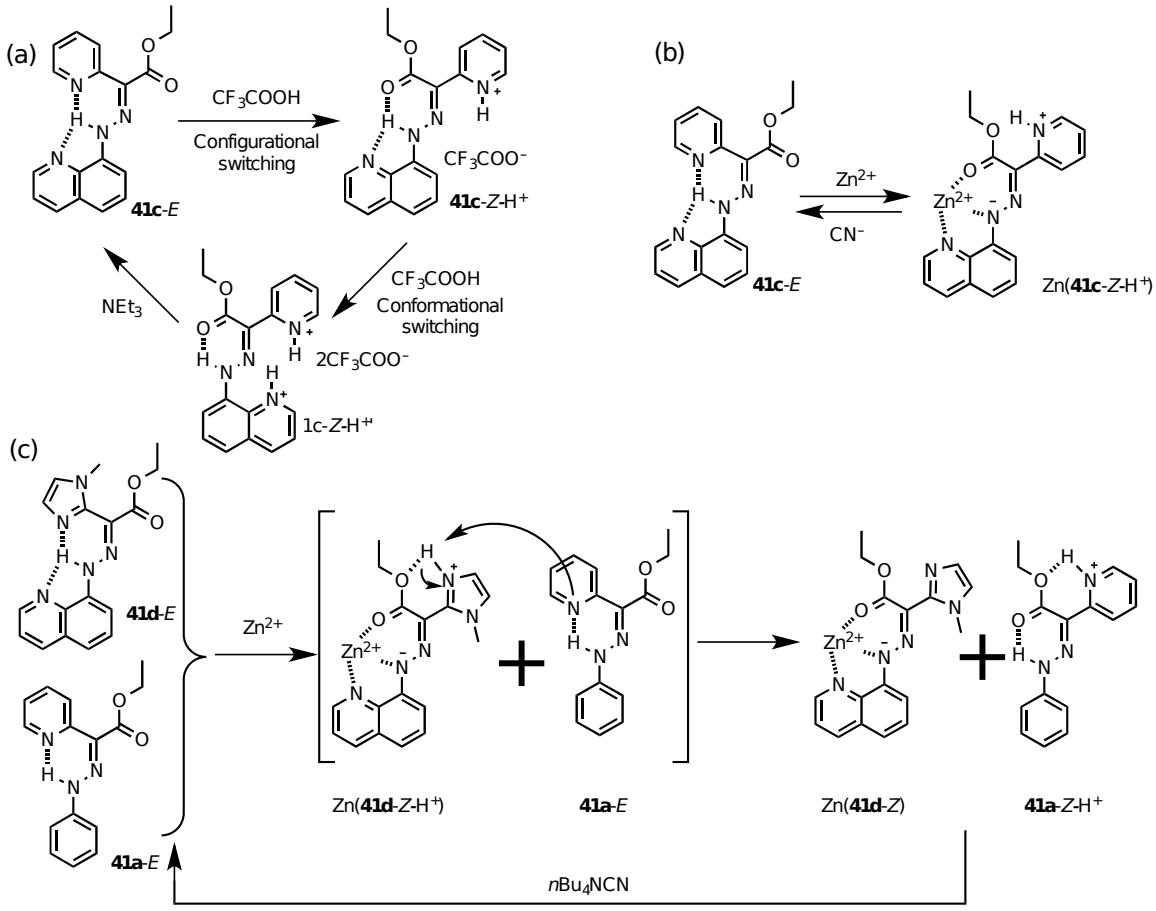

Figure 17. Modified hydrazone switches (a) a configurational and conformational switch activated by stepwise protonation, (b) a reversible switching activated by CCD mechanism, (c) cascade switching based on the CCD mechanism.

3. Molecular Machines Operated by DCC

Reversible covalent changes could be built within artificial molecular machines and utilized subsequently to direct controllable molecular

motional changes, provided that the related covalent bonds can break and reform with high specificity under mild chemical environment. The covalent characteristics should endow distinctive chemical states and thus bring high selectivity to their function. As summarized below, delicate design has led to great advancement of artificial molecular machines that are operated under reversible DCC conditions.

3.1 Molecular Shuttles

Leigh and coworkers demonstrated an example of a bistable molecular shuttle that functioned through the formation and breaking of C–C bonds by virtue of the well-established reversible Diels–Alder reaction (Figure 18).[58] The [2]rotaxane **42**-A was constructed to contain two stations, one diamide derived from fumaric acid (Station I) and one monoamide monoester derived from succinic acid (Station II), on the dumbbell-shaped component. A tetraamide macrocycle was selectively located on Station I due to stronger H-bonding interactions with fumaramide. Treating [2]rotaxane **42**-A with cyclopentadiene (CP) at 80 °C triggered its Diels-Alder cycloaddition to the double bond of Station I, resulting in shuttling of the tetraamide macrocycle from Station I to Station II. When the CP-appended [2]rotaxane **42**-B was heated at 250 °C under reduced pressure, retro-Diels-Alder reaction took place. The recovered Station I once again became the preferred recognition unit for the movable macrocycle, and the original state was restored.

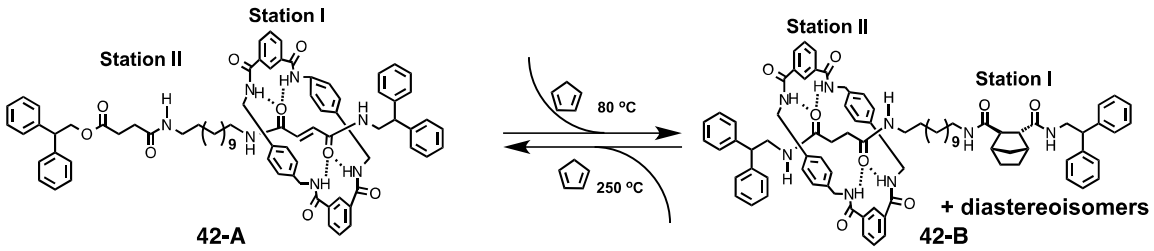

Figure 18. Switching of molecular shuttle **42** by reversible D-A reaction.

Suzuki and coworkers have constructed bis-imine [2]rotaxanes **43a/b** that contained a macrocycle with two amino groups and a bisaldehyde dumbbell component (Figure 19a).[59] The macrocycle was affixed to the central bisaldehyde moiety due to the formation of imine bonds. When **43a** was subjected to acidic hydrolysis conditions, stepwise imine dissociation was triggered. Corresponding aldehyde-ammonium-monoimine (B in Figure 19b) and dialdehyde-diammonium rotaxanes (C in Figure 19b) could be identified, the latter of which allowed the macrocycle shuttling between two identical *p*-$OCH_2C_6H_4CH_2O$ spacers. The ratio of the dialdehyde-diammonium rotaxane increased upon decreasing the temperature between 40 °C and –40 °C, suggesting that the imine hydrolysis is enthalpy-driven while the imine bond formation is entropy-driven. This example thus demonstrated that submolecular mobility of the relative components

could be controlled through temperature dependent reversible imine formation.

Interestingly, when triethylene glycol spacers were used in **43b** in replacement of the *p*-$OCH_2C_6H_4CH_2O$ ones in **43a**, the formation of intermediate aldehyde-ammonium-monoimine rotaxane was highly disfavored during hydrolysis.[60] Instead, the equilibrium was displaced towards the dialdehyde-diammonium rotaxane due to favorable hydrogen bonding between ammonium and the triethyleneglycol ether unit (Figure 19b). In contrast to [2]rotaxane **43a**, which behaves as a shuttle equilibrating between two identical states, in [2]rotaxane **43b** the shuttling is suppressed due to same intramolecular H-bonding interactions. The hydrating/dehydrating process could also be exercised by temperature control. At 100 °C under hydrolytic conditions, there was more than 95% bisimine [2]rotaxane, while at 0 °C there was 95% fully hydrolyzed [2]rotaxane, suggesting that this molecule could function as a molecular shuttle exhibiting entropy-driven translational isomerism with remarkable positional discrimination.

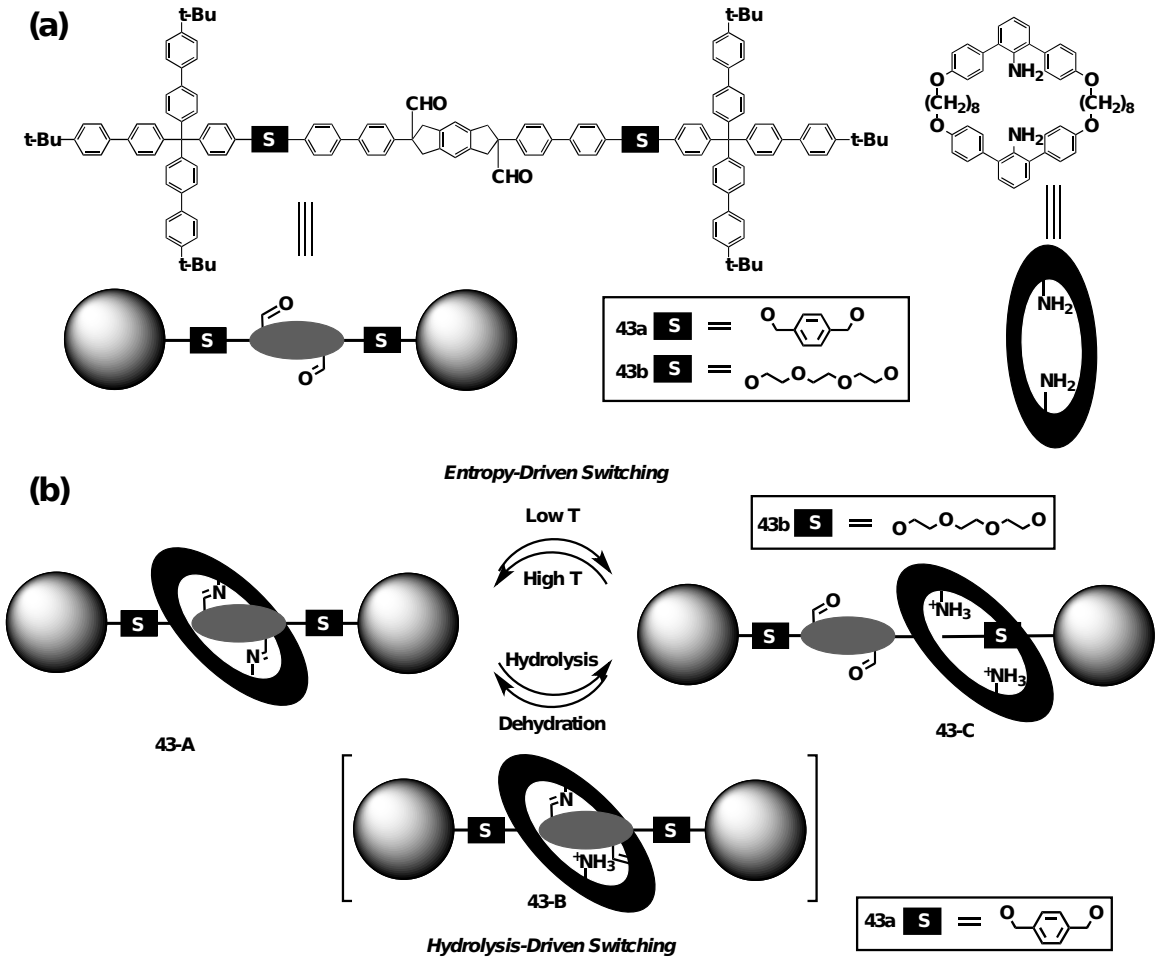

Figure 19. (a) Molecular structures of components of Suzuki's [2]rotaxanes **43a** and **43b**. (b) Illustration of the acid and temperature dependent switching of the molecular shuttles.

3.2. Molecular Walkers

Molecular walkers, which could be regarded as a special class of molecular motors, refer to the molecular systems where part of the molecules could move from one position to another after a series of chemical operations, similar to movements that walk along a track.[61] The first synthetic molecular walker was reported by Leigh and

coworkers.[62] The molecule **44** consisted of a molecular track and a walker unit that was covalently linked by two different types of dynamic covalent bonds, namely, hydrazone and disulfide linkages (Figure 20). The molecular track could be described as a four-station track, two of which were for hydrazone formation and the other were for disulfides, arranged alternatingly along the molecular backbone. Under acidic conditions, the macrocycle connecting stations **1** and **2** opened up at station **1** due to hydrazone hydrolysis. Under this equilibrating condition, hydrazone was formed at station **3** to give a new constitutional isomer, which corresponded to a first step moving of the walker along the track, with the other foot remaining locked on station **2** by S-S disulfide bond. The next walking step was activated by base, under which conditions the hydrazone foot at station **3** remained locked while the disulfide foot was unchained and allowed to complete the next step by reforming a new disulfide bond at station **4**. Such acid-base activation drove the walker to move from stations **1** and **2** to station **3** and **4**. All of the reactions employed in the operation of this walker-track were equilibrium-based DCC reactions, thus the walker unit moved back and forth along the track between chemically equivalent footholds, i.e., the directionality was not well controlled. As a result, the final equilibrated systems consisted of a mixture of isomers, including 1,4-isomers and these intermediate walker-track systems, the ratio of which were related to the acid-base conditions. In

an improved system,[63] the walker could be made more preferentially along one direction by using an extra irreversible oxidation step to give rise more of the completed walker-tracker 3,4-isomer in the equilibrated system.

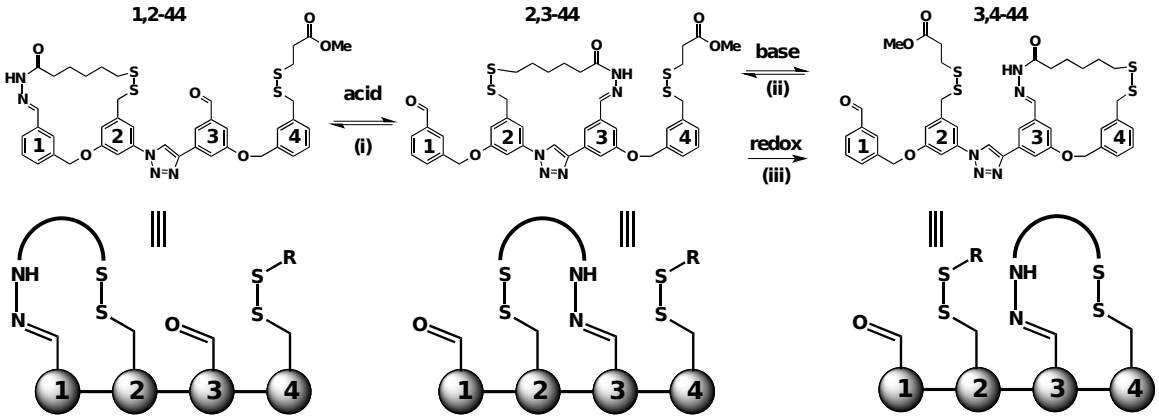

Figure 20. Illustration of the processive molecular walker **44** walking along the track via a series of DCC reactions.

The directionality, i.e., the product distribution between the isomers, was further improved significantly when an photoresponsive stilbene unit was incorporated in between two of the stations.[64] As shown in Figure 21, in the initial state of molecular walker **45**, the stilbene unit adopted an *E*-form. The directional migration of the walker unit from 1,2-isomer to 2,3-isomer was promoted by the following series of operations — after photochemical *E*-*Z* isomerization, the base activation step was applied to trigger the re-equilibrium of the walker between *Z*-1,2-**45** and *Z*-2,3-**45** with a ratio of 40:60. Subsequent photoisomerization of the *Z*-2,3-**45** walker gave the

corresponding *E*-2,3-**45**, which also induced a strain within the walker macrocycle. The following acyl-hydrazone exchange could be activated by TFA hydrolysis to give *E*-3,4-**45**, which was greatly favored as driven by strain in *E*-2,3-**45**. This step was now furnished with a much enhanced selectivity (>95:5) towards the formation of *E*-3,4-**45**. The combined photoisomerization and acid-base activation steps could be used to reverse the walker-track migration sequence, thus endowed much improved processive and directional stepping.

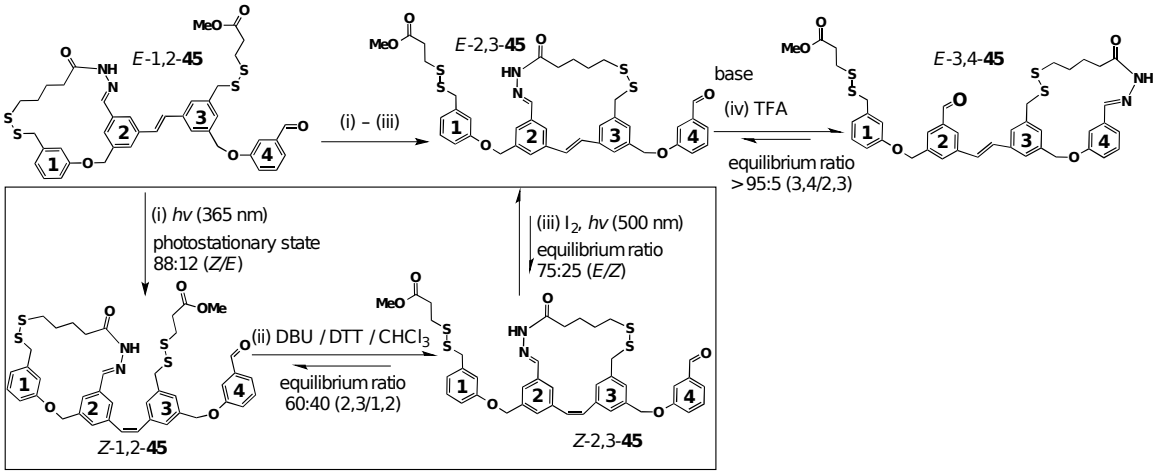

Figure 21. A light driven molecular walker **45**. The reactions highlighted in the box are breakdown steps for the formal walking steps from *E*-1,2-**45** to *E*-2,3-**45.**

Aside from these linear walkers, an elegant, biomimetic, interlocked molecular walker that also functioned as a peptide synthesizer was recently reported by Leigh and co-workers,[65] which was reminiscent of ribosomal protein synthesis in biological systems. In

this [2]rotaxane **46**, a macrocycle walker can move along a linear thread, which contains several amino acid-appended stations, while carrying a catalytic thiolate group. As the walker moves along the axial thread of the [2]rotaxane, it goes through several capture-rearrangement steps that ultimately lead to an autonomous peptide synthesis process in a sequence-specific manner (Figure 22).

In [2]rotaxane **46**, the macrocyclic hydrazone walker was constructed to bear a cysteine unit with a trityl-protected thiolate group, and the axial component contained three different Boc-protected amino acid units that were separated from each other by rigid spacers. At the initial state, the macrocycle was located on the segments between the terminal stopper and the Boc-phenylalanine ester group. Activation of the walker was initiated by acid, which effectively liberated the free thiol and amino units after cleavage of trityl and Boc protecting groups to give **47** (step 1). Upon treatment with *N*,*N*-diisopropylethylamine, the thiol was deprotonated to become an active thiolate catalyst, which reacted with the nearby phenylalanine phenolic ester through transacylation reaction (step 2). The transferred phenylalanine unit was further relocated to the end of the macrocycle through an intramolecular 1,11-*S*,*N*-acyl transfer process (step 3), ending up with regeneration of the active thiolate site and elongation of peptide sequence on the macrocycle. Once the first aminoacid building block was removed, the macrocycle walker could

now move further along the track to reach the second aminoacid building block. Another cycle of *O*-*S* transacylation and subsequent 1,14-*S,N*-acyl transfer steps (step 4) furnished the second peptide elongation process. Finally, one more repetitive sequential acyl transfer (step 5) completed the third elongation step. Dissociation of the macrocycle walker from the axial thread occurred after the removal of the last amino acid stopper, which, upon hydrazone hydrolysis, gave the sequence-specific hydrazide peptide **49** (step 6). Remarkably, no starting material, deletions, or unexpected sequences were observed, highlighting the accuracy of the autonomous actions. Overall, a combination of transacylation reaction, thiolate regeneration and macrocycle walking was employed to generate a synthetic system that could function as an autonomous peptide synthesizer.

The above [2]rotaxane molecular walker was synthesized by a “final-step-threading” method, which relied on a key active template reaction as the last step of a long synthetic route. The low yield of the final threading limited its utility for longer peptide synthesis. This situation was significantly improved by utilizing a “rotaxane-capping” protocol, which involved attachment of a preformed [2]rotaxane synthon to the end of a fully formed strand of building blocks.[66] Threaded molecular machines with extended oligomeric, and potentially polymeric tracks could be obtained following this protocol. Despite some limitations, such as slow kinetics and loss of the

sequence information on the track during its working, such a molecular walker represents an important step towards the fabrication of artificial molecular machines that can perform complex work comparable to nature's biological machines.

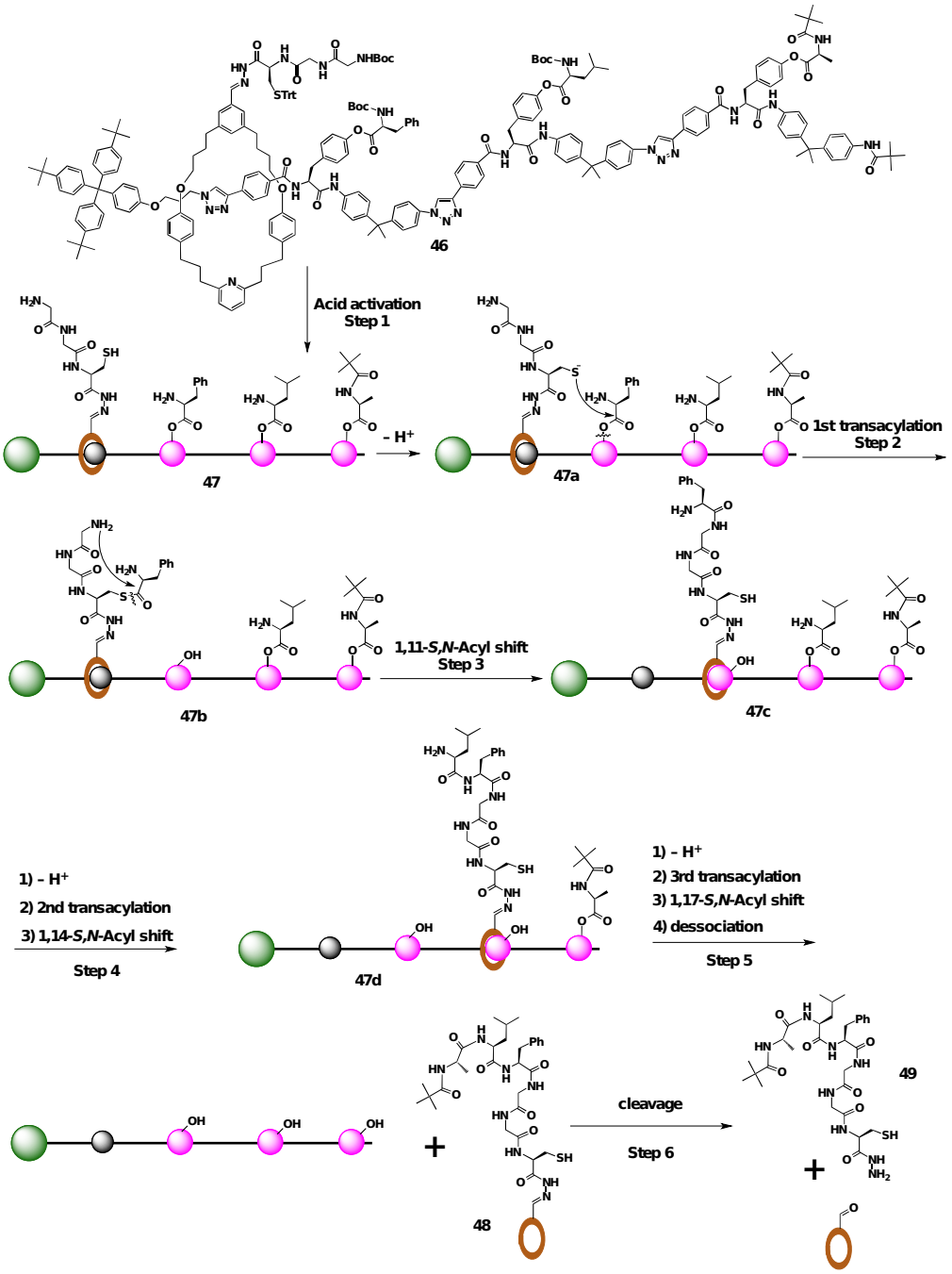

Figure 22. A [2]rotaxane based molecular walker **46** that synthesizes

peptide **49** after a sequence of capture-rearrangement steps.

Lehn and coworkers have described[67] a simple prototype of system that displays relative motions of molecular moieties based on imine exchange within the reaction between salicylaldehyde (SALAL) and linear oligoamines (Figure 23). For example, the 1:1 condensation product of SALAL and diethylene triamine gave **49**, in which nondirectional displacement occurred as the aldehyde residue transferred along the polyamine chain by reversible covalent bond formation. As indicated in Figure 23, cyclic aminal and iminium intermediates were formed during the intramolecular inchworm-like movement of a salicylidene residue along the oligoamine chain, which was processive since the two moieties remained attached along the way. Such motional processes take place without change in molecular constitution, thus representing a novel category of dynamic covalent motions.

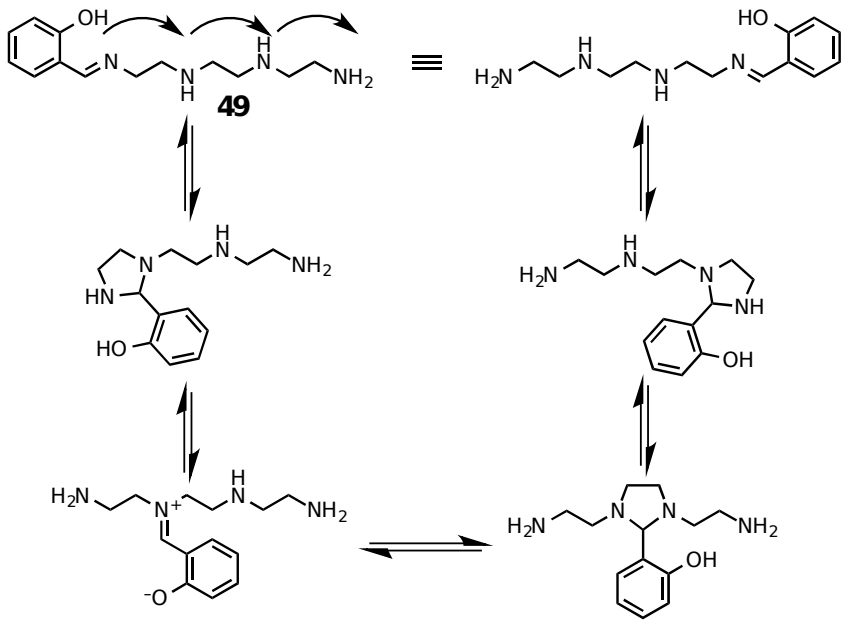

Figure 23. Mechanism of the dynamic intramolecular inchworm-type walking of a salicylidene residue along an oligoamine chain.

The above imine-based molecular walker showcases a simple prototype of processive machines, despite that the movement lacks directionality. In an improved design, controlled directional displacement of a molecular group has been achieved.[68] It was based on the reactions of *ortho*-carboxybenzaldehyde (CAXAL) with primary and secondary amines to give imines or amino lactones, respectively, depending on the acidity of the medium. When there was also a formyl group *ortho* to the hydroxyl, such as 2-formyl-3-hydroxybenzoic acid (SAXAL), it combined the structural benefits of both salicylaldehyde (SALAL), which preferred imine formation, and CAXAL, which preferred

formation of lactone under acidic conditions. With the control of pH, the intramolecular walker **50** (Figure 24) could thus be programmed to have the SAXAL unit walk along a non-symmetric polyamine chain, with an imine serving as the terminus under basic conditions on one end and a lactone formed on the other end under acidic conditions. In other words, the lactone **51** was formed quantitatively upon reacting SAXAL under acidic conditions with the track in its free base form. Addition of three equivalents of base was required to shift the equilibrium to the imine form **50**. The displacement was fully reversible and addition of three equivalents of acid reverted the displacement completely to the starting lactone **51**. By utilizing the special reactivity of the *ortho*-carboxybenzaldehyde, this dynamic covalent motional system extends the DCC of imines to secondary amines, and could open up new perspectives in this field.

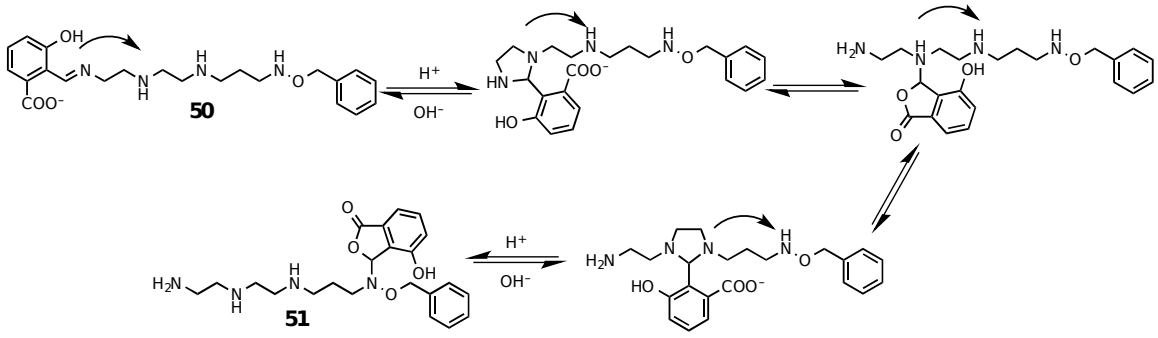

Figure 24. Displacement of the SAXAL walker along the polyamine track bearing a primary amine as the imine-forming terminus and the benzoxyamine as the lactone terminus.

In addition to imine chemistry, a molecular walker was constructed by Leigh and coworkers based on processive intramolecular Michael and Retro-Michael reactions.[69] As shown in Figure 25, a model walker-track conjugate **52** was designed to contain a α-methylene-4-nitrostyrene walking unit and an oligoethyleneimine track. The walking unit was initially linked to the first amine foothold of the track by one leg. Subsequent ring closing intramolecular Michael addition reaction between the olefin bond of the styrene unit and the adjacent amine group of the track resulted in attachment of the walking unit to a neighboring foothold. Following a retro-Michael ring opening rearrangement reaction, either legs of the walking unit were detached from the track, leaving a free, reactive olefin bond ready for repetitive foothold attachment and detachment sequences. Such a sequence allowed a α-methylene-4-nitrostyrene walker to travel through five footholds along the track step without external intervention. When an anthracene fluorophore was installed on the opposite end of the walker unit along the oligoethyleneimine track, 54% quenching of anthracene fluorescence was observed in **53** after a thermodynamic equilibrium was reached within 6.5 hours, corresponding to an intramolecular static quenching effect imposed by the nitrostyrene walker that was closer in space after walking back and forth along the track. Recently, the α-methylene-4-nitrostyrene walker was shown to be able to walk along an oligoethyleneimine track with

up to nine footholds with a naphthylmethylamine end.[70] Interestingly, naphthylmethylamine appeared to be the most favorable foothold for the walker, with the dynamics of the walker migration following random walk of a Brownian particle in one dimension.

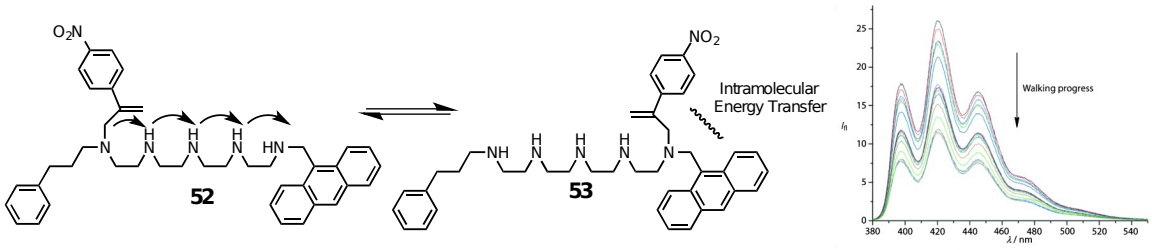

Figure 25. A processive walker based on Michael-retro-Michael addition mechanism that can perform a simple task, i.e., quenching the fluorescence of the end anthracene group.

4. Concluding Remarks and Outlook

The marriage of DCC and molecular machines has undoubted brought new opportunities to the field of artificial molecular machines. On one hand, design and synthesis of rather complex metastable molecular systems could benefit from the high selectivity and specificity aspects of DCC chemistry. On the other hand, employment of DCC chemistry opens the door to build molecular machineries with unconventional switching pathways that rely on constitutional changes in addition to *co*-conformational changes. Furthermore, operation of molecular machines by covalent bonding changes offers more distinctive states, implying more functions and controllability. Finally, as having been

manifested in synthetic molecular walkers, the use of orthogonal DCC chemistry enables the fabrication of more sophisticated artificial molecular machines. These machines take advantage of the dynamic nature of reversible reactions, which is distinctive from these based on noncovalent interactions. Most of the systems, however, rely on thermodynamically equilibrated systems. This leaves a lot of room for future studies of the kinetics of molecular machineries. Any chemical input, or input by other means that can affect the equilibrium, for example, kinetic fixation of a dynamic covalent bond, will be useful in enhancing the operation efficacy of such machines.

From a practical point of view, transforming molecular machines from chemical devices to mechanical devices that can accomplish real world tasks is one of the most pressing tasks in contemporary nanoscience.[71] Scientists have made great strides in instating bistabilities in molecular systems, yet how to integrate these switchable molecules into hierarchical and coherent suprastructures to perform work on their immediate environment across different length scales, is still a grand challenge. On the single molecular level, how these machines respond to thermal fluctuation is fundamental to the understanding of basic molecular behavior. The fusion of DCC and molecular machines naturally opens up the window to the discoveries of biomimetic materials systems with controls that are on par to or superior than nature’s machines. The versatile features associated

with synthetic molecular machines, which in many cases are inaccessible without the enabling DCC chemistry, will continue to provide an informed search for more functional chemical devices and a pathway to real world mechanical devices.

5. References

(1) Sauvage, J.-P. Transition Metal-Containing Rotaxanes and Catenanes in Motion: Toward Molecular Machines and Motors. *Acc. Chem. Res.* **1998**, *31*, 611-619.
(2) Balzani, V.; Credi, A.; Raymo, F. M.; Stoddart, J. F. Artificial Molecular Machines. *Angew. Chem. Int. Ed.* **2000**, *39*, 3348-3391.
(3) Balzani, V.; Credi, A.; Venturi, M. In *Molecular Devices and Machines – a Journey into the Nano World*; Wiley-VCH Verlag GmbH & Co. KGaA: 2004.
(4) Kay, E. R.; Leigh, D. A. Rise of the Molecular Machines. *Angew. Chem. Int. Ed.* **2015**, *54*, 10080-10088.
(5) Mavroidis, C.; Dubey, A.; Yarmush, M. Molecular Machines. *Annu. Rev. Biomed. Eng.* **2004**, *6*, 363-395.
(6) Stoddart, J. F. Putting Mechanically Interlocked Molecules (Mims) to Work in Tomorrow's World. *Angew. Chem. Int. Ed.* **2014**, *53*, 11102-11104.
(7) Lehn, J. M. Perspectives in Supramolecular Chemistry—from Molecular Recognition Towards Molecular Information Processing and Self-Organization. *Angew. Chem. Int. Ed. Engl.* **1990**, *29*, 1304-1319.
(8) Lehn, J.-M. *Supramolecular Chemistry*; Vch, Weinheim, 1995; Vol. 1.
(9) Steed, J. W.; Atwood, J. L. *Supramolecular Chemistry*; John Wiley & Sons, 2013.
(10) Rowan, S. J.; Cantrill, S. J.; Cousins, G. R. L.; Sanders, J. K. M.; Stoddart, J. F. Dynamic Covalent Chemistry. *Angew. Chem. Int. Ed.* **2002**, *41*, 898-952.
(11) Lehn, J.-M. From Supramolecular Chemistry Towards Constitutional Dynamic Chemistry and Adaptive Chemistry. *Chem. Soc. Rev.* **2007**, *36*, 151-160.
(12) Jin, Y.; Yu, C.; Denman, R. J.; Zhang, W. Recent Advances in Dynamic Covalent Chemistry. *Chem. Soc. Rev.* **2013**, *42*, 6634-6654.
(13) Wilson, A.; Gasparini, G.; Matile, S. Functional Systems with Orthogonal Dynamic Covalent Bonds. *Chem. Soc. Rev.* **2014**, *43*, 1948-1962.
(14) Rue, N. M.; Sun, J.; Warmuth, R. Polyimine Container Molecules and Nanocapsules. *Isr. J. Chem.* **2011**, *51*, 743-768.

(15) Corbett, P. T.; Leclaire, J.; Vial, L.; West, K. R.; Wietor, J.-L.; Sanders, J. K. M.; Otto, S. Dynamic Combinatorial Chemistry. *Chem. Rev.* **2006**, *106*, 3652-3711.
(16) Otto, S.; Severin, K. Dynamic Combinatorial Libraries for the Development of Synthetic Receptors and Sensors. *Top. Curr. Chem.* **2007**, *277*, 267-288.
(17) Li, J.; Nowak, P.; Otto, S. Dynamic Combinatorial Libraries: From Exploring Molecular Recognition to Systems Chemistry. *J. Am. Chem. Soc.* **2013**, *135*, 9222-9239.
(18) Stadler, A.-M.; Ramirez, J. Synthetic Molecular Machines and Polymer/Monomer Size Switches That Operate through Dynamic and Non-Dynamic Covalent Changes. *Top. Curr. Chem.* **2012**, *322*, 261-290.
(19) Liu, Y.; Li, Z.-T. A Dynamic Route to Structure and Function: Recent Advances in Imine-Based Organic Nanostructured Materials. *Aust. J. Chem.* **2013**, *66*, 9-22.
(20) Haussmann, P. C.; Stoddart, J. F. Synthesizing Interlocked Molecules Dynamically. *Chem. Rec.* **2009**, *9*, 136-154.
(21) Glink, P. T.; Oliva, A. I.; Stoddart, J. F.; White, A. J. P.; Williams, D. J. Template-Directed Synthesis of a [2]Rotaxane by the Clipping under Thermodynamic Control of a Crown Ether Like Macrocycle around a Dialkylammonium Ion. *Angew. Chem. Int. Ed.* **2001**, *40*, 1870-1875.
(22) Wu, J.; Leung, K. C.-F.; Stoddart, J. F. Efficient Production of N Rotaxanes by Using Template-Directed Clipping Reactions. *Proc. Natl. Acad. Sci. U. S. A.* **2007**, *104*, 17266-17271.
(23) Belowich, M. E.; Valente, C.; Smaldone, R. A.; Friedman, D. C.; Thiel, J.; Cronin, L.; Stoddart, J. F. Positive Cooperativity in the Template-Directed Synthesis of Monodisperse Macromolecules. *J. Am. Chem. Soc.* **2012**, *134*, 5243-5261.
(24) Coronado, E.; Gavina, P.; Ponce, J.; Tatay, S. Fast Pirouetting Motion in a Pyridine Bisamine-Containing Copper-Complexed Rotaxane. *Chem. - Eur. J.* **2014**, *20*, 6939-6950.
(25) Li, Z.; Hu, F.; Liu, G.; Xue, W.; Chen, X.; Liu, S. H.; Yin, J. Photo-Responsive [2]Catenanes: Synthesis and Properties. *Org. Biomol. Chem.* **2014**, *12*, 7702-7711.
(26) Wong, W.-Y.; Leung, K. C.-F.; Stoddart, J. F. Self-Assembly, Stability Quantification, Controlled Molecular Switching, and Sensing Properties of an Anthracene-Containing Dynamic 2 Rotaxane. *Org. Biomol. Chem.* **2010**, *8*, 2332-2343.
(27) Klivansky, L. M.; Koshkakaryan, G.; Cao, D.; Liu, Y. Linear Π-Acceptor-Templated Dynamic Clipping to Macrobicycles and [2]Rotaxanes. *Angew. Chem. Int. Ed.* **2009**, *48*, 4185-4189.
(28) Pun, A.; Hanifi, D. A.; Kiel, G.; O'Brien, E.; Liu, Y. Facile Route to an All-Organic, Triply Threaded, Interlocked Structure by Templated Dynamic Clipping. *Angew. Chem.* **2012**, *124*, 13296-13299.

(29) Pun, A. B.; Gagnon, K. J.; Klivansky, L. M.; Teat, S. J.; Li, Z.-T.; Liu, Y. Solvent-Driven Selective Π-Cation Templating in Dynamic Assembly of Interlocked Molecules. *Org. Chem. Front.* **2014**, *1*, 167-175.
(30) Koshkakaryan, G.; Cao, D.; Klivansky, L. M.; Teat, S. J.; Tran, J. L.; Liu, Y. Dual Selectivity Expressed in [2 + 2 + 1] Dynamic Clipping of Unsymmetrical [2]Catenanes. *Org. Lett.* **2010**, *12*, 1528-1531.
(31) Lam, R. T. S.; Belenguer, A.; Roberts, S. L.; Naumann, C.; Jarrosson, T.; Otto, S.; Sanders, J. K. M. Amplification of Acetylcholine-Binding Catenanes from Dynamic Combinatorial Libraries. *Science* **2005**, *308*, 667-669.
(32) Au-Yeung, H. Y.; Pantos, G. D.; Sanders, J. K. M. Amplifying Different [2]Catenanes in an Aqueous Donor-Acceptor Dynamic Combinatorial Library. *J. Am. Chem. Soc.* **2009**, *131*, 16030-16031.
(33) Au-Yeung, H. Y.; Pantos, G. D.; Sanders, J. K. M. Dynamic Combinatorial Synthesis of a Catenane Based on Donor-Acceptor Interactions in Water. *Proc. Natl. Acad. Sci. U. S. A.* **2009**, *106*, 10466-10470.
(34) Au-Yeung, H. Y.; Pantos, G. D.; Sanders, J. K. M. A Water Soluble Donor-Acceptor [2]Catenane That Can Switch between a Coplanar and a Gemini-Sign Conformation. *Angew. Chem. Int. Ed.* **2010**, *49*, 5331-5334.
(35) Cougnon, F. B. L.; Jenkins, N. A.; Pantoş, G. D.; Sanders, J. K. M. Templated Dynamic Synthesis of a [3]Catenane. *Angew. Chem. Int. Ed.* **2012**, *51*, 1443-1447.
(36) Black, S. P.; Stefankiewicz, A. R.; Smulders, M. M. J.; Sattler, D.; Schalley, C. A.; Nitschke, J. R.; Sanders, J. K. M. Generation of a Dynamic System of Three-Dimensional Tetrahedral Polycatenanes. *Angew. Chem. Int. Ed.* **2013**, *52*, 5749-5752.
(37) Cougnon, F. B. L.; Au-Yeung, H. Y.; Pantoş, G. D.; Sanders, J. K. M. Exploring the Formation Pathways of Donor−Acceptor Catenanes in Aqueous Dynamic Combinatorial Libraries. *J. Am. Chem. Soc.* **2011**, *133*, 3198-3207.
(38) Cantrill, S. J.; Grubbs, R. H.; Lanari, D.; Leung, K. C. F.; Nelson, A.; Poulin-Kerstien, K. G.; Smidt, S. P.; Stoddart, J. F.; Tirrell, D. A. Template-Directed Olefin Cross Metathesis. *Org. Lett.* **2005**, *7*, 4213-4216.
(39) Guidry, E. N.; Li, J.; Stoddart, J. F.; Grubbs, R. H. Bifunctional C2 Daisy-Chains and Their Incorporation into Mechanically Interlocked Polymers. *J. Am. Chem. Soc.* **2007**, *129*, 8944-8945.
(40) Guidry, E. N.; Cantrill, S. J.; Stoddart, J. F.; Grubbs, R. H. Magic Ring Catenation by Olefin Metathesis. *Org. Lett.* **2005**, *7*, 2129-2132.
(41) Li, S.; Liu, M.; Zheng, B.; Zhu, K.; Wang, F.; Li, N.; Zhao, X.-L.; Huang, F. Taco Complex Templated Syntheses of a Cryptand/Paraquat [2]Rotaxane and a [2]Catenane by Olefin Metathesis. *Org. Lett.* **2009**, *11*, 3350-3353.

(42) Badjić, J. D.; Cantrill, S. J.; Grubbs, R. H.; Guidry, E. N.; Orenes, R.; Stoddart, J. F. The Exclusivity of Multivalency in Dynamic Covalent Processes. *Angew. Chem. Int. Ed.* **2004**, *43*, 3273-3278.
(43) Wang, L.; Vysotsky, M. O.; Bogdan, A.; Bolte, M.; Böhmer, V. Multiple Catenanes Derived from Calix[4]Arenes. *Science* **2004**, *304*, 1312-1314.
(44) Zhu, X.-Z.; Chen, C.-F. A Highly Efficient Approach to [4]Pseudocatenanes by Threefold Metathesis Reactions of a Triptycene-Based Tris[2]Pseudorotaxane. *J. Am. Chem. Soc.* **2005**, *127*, 13158-13159.
(45) Hou, H.; Leung, K. C. F.; Lanari, D.; Nelson, A.; Stoddart, J. F.; Grubbs, R. H. Template-Directed One-Step Synthesis of Cyclic Trimers by Admet. *J. Am. Chem. Soc.* **2006**, *128*, 15358-15359.
(46) Dietrich-Buchecker, C.; Rapenne, G. Efficient Synthesis of a Molecular Knot by Copper(I)-Induced Formation of the Precursor Followed by Ruthenium(Ii)-Catalysed Ring Closing Metathesis. *Chem. Commun.* **1997**, 2053-2054.
(47) Ayme, J.-F.; Gil-Ramírez, G.; Leigh, D. A.; Lemonnier, J.-F.; Markevicius, A.; Muryn, C. A.; Zhang, G. Lanthanide Template Synthesis of a Molecular Trefoil Knot. *J. Am. Chem. Soc.* **2014**, *136*, 13142-13145.
(48) Leigh, D. A.; Pritchard, R. G.; Stephens, A. J. A Star of David Catenane. *Nat. Chem.* **2014**, *6*, 978-982.
(49) Meng, Z.; Han, Y.; Wang, L.-N.; Xiang, J.-F.; He, S.-G.; Chen, C.-F. Stepwise Motion in a Multivalent [2](3)Catenane. *J. Am. Chem. Soc.* **2015**, *137*.
(50) Asakawa, M.; Ashton, P. R.; Balzani, V.; Credi, A.; Hamers, C.; Mattersteig, G.; Montalti, M.; Shipway, A. N.; Spencer, N.; Stoddart, J. F.; Tolley, M. S.; Venturi, M.; White, A. J. P.; Williams, D. J. A Chemically and Electrochemically Switchable [2]Catenane Incorporating a Tetrathiafulvalene Unit. *Angew. Chem. Int. Ed.* **1998**, *37*, 333-337.
(51) van Delden, R. A.; ter Wiel, M. K. J.; Pollard, M. M.; Vicario, J.; Koumura, N.; Feringa, B. L. Unidirectional Molecular Motor on a Gold Surface. *Nature* **2005**, *437*, 1337-1340.
(52) Lehn, J.-M. Conjecture: Imines as Unidirectional Photodriven Molecular Motors—Motional and Constitutional Dynamic Devices. *Chem. Eur. J.* **2006**, *12*, 5910-5915.
(53) Leung, K. C.-F.; Xuan, S.; Lo, C.-M. Reversible Switching between Hydrophilic and Hydrophobic Superparamagnetic Iron Oxide Microspheres Via One-Step Supramolecular Dynamic Dendronization: Exploration of Dynamic Wettability. *ACS Appl. Mater. Inter.* **2009**, *1*, 2005-2012.
(54) Landge, S. M.; Tkatchouk, E.; Benítez, D.; Lanfranchi, D. A.; Elhabiri, M.; Goddard, W. A.; Aprahamian, I. Isomerization Mechanism in Hydrazone-Based Rotary Switches: Lateral Shift, Rotation, or Tautomerization? *J. Am. Chem. Soc.* **2011**, *133*, 9812-9823.

(55) Su, X.; Aprahamian, I. Switching around Two Axles: Controlling the Configuration and Conformation of a Hydrazone-Based Switch. *Org. Lett.* **2011**, *13*, 30-33.
(56) Su, X.; Robbins, T. F.; Aprahamian, I. Switching through Coordination-Coupled Proton Transfer. *Angew. Chem. Int. Ed.* **2011**, *50*, 1841-1844.
(57) Ray, D.; Foy, J. T.; Hughes, R. P.; Aprahamian, I. A Switching Cascade of Hydrazone-Based Rotary Switches through Coordination-Coupled Proton Relays. *Nat Chem* **2012**, *4*, 757-762.
(58) Leigh, D. A.; Perez, E. M. Shuttling through Reversible Covalent Chemistry. *Chem. Commun.* **2004**, 2262-2263.
(59) Kawai, H.; Umehara, T.; Fujiwara, K.; Tsuji, T.; Suzuki, T. Dynamic Covalently Bonded Rotaxanes Cross-Linked by Imine Bonds between the Axle and Ring: Inverse Temperature Dependence of Subunit Mobility. *Angew. Chem. Int. Ed.* **2006**, *45*, 4281-4286.
(60) Umehara, T.; Kawai, H.; Fujiwara, K.; Suzuki, T. Entropy- and Hydrolytic-Driven Positional Switching of Macrocycle between Imine- and Hydrogen-Bonding Stations in Rotaxane-Based Molecular Shuttles. *J. Am. Chem. Soc.* **2008**, *130*, 13981-13988.
(61) von Delius, M.; Leigh, D. A. Walking Molecules. *Chem. Soc. Rev.* **2011**, *40*, 3656-3676.
(62) von Delius, M.; Geertsema, E. M.; Leigh, D. A. A Synthetic Small Molecule That Can Walk Down a Track. *Nat. Chem.* **2010**, *2*, 96-101.
(63) von Delius, M.; Geertsema, E. M.; Leigh, D. A.; Tang, D.-T. D. Design, Synthesis, and Operation of Small Molecules That Walk Along Tracks. *J. Am. Chem. Soc.* **2010**, *132*, 16134-16145.
(64) Barrell, M. J.; Campana, A. G.; von Delius, M.; Geertsema, E. M.; Leigh, D. A. Light-Driven Transport of a Molecular Walker in Either Direction Along a Molecular Track. *Angew. Chem. Int. Ed.* **2011**, *50*, 285-290.
(65) Lewandowski, B.; De Bo, G.; Ward, J. W.; Papmeyer, M.; Kuschel, S.; Aldegunde, M. J.; Gramlich, P. M. E.; Heckmann, D.; Goldup, S. M.; D'Souza, D. M.; Fernandes, A. E.; Leigh, D. A. Sequence-Specific Peptide Synthesis by an Artificial Small-Molecule Machine. *Science* **2013**, *339*, 189-193.
(66) De Bo, G.; Kuschel, S.; Leigh, D. A.; Lewandowski, B.; Papmeyer, M.; Ward, J. W. Efficient Assembly of Threaded Molecular Machines for Sequence-Specific Synthesis. *J. Am. Chem. Soc.* **2014**, *136*, 5811-5814.
(67) Kovaříček, P.; Lehn, J.-M. Merging Constitutional and Motional Covalent Dynamics in Reversible Imine Formation and Exchange Processes. *J. Am. Chem. Soc.* **2012**, *134*, 9446-9455.
(68) Kovaříček, P.; Lehn, J.-M. Directional Dynamic Covalent Motion of a Carbonyl Walker on a Polyamine Track. *Chem. Eur. J.* **2015**, *21*, 9380-9384.
(69) Campaña, A. G.; Carlone, A.; Chen, K.; Dryden, D. T. F.; Leigh, D. A.; Lewandowska, U.; Mullen, K. M. A Small Molecule That Walks Non-

Directionally Along a Track without External Intervention. *Angew. Chem. Int. Ed.* **2012**, *51*, 5480-5483.
(70) Campaña, A. G.; Leigh, D. A.; Lewandowska, U. One-Dimensional Random Walk of a Synthetic Small Molecule toward a Thermodynamic Sink. *J. Am. Chem. Soc.* **2013**, *135*, 8639-8645.
(71) Coskun, A.; Banaszak, M.; Astumian, R. D.; Stoddart, J. F.; Grzybowski, B. A. Great Expectations: Can Artificial Molecular Machines Deliver on Their Promise? *Chem. Soc. Rev.* **2012**, *41*, 19-30.